GAP FORMATION BETWEEN STEEL LINER AND CYLINDER WALL IN REACTOR CONTAINMENT

REPORT 2026:1181

NUCLEAR POWER CONCRETE TECHNOLOGY

Energiforsk

Gap formation between steel liner and cylinder wall in reactor containment buildings

NILS JANESTAD, MANOUCHEHR HASSANZADEH, CAMILO RITO PI AND ELIN TORÉN JOHANSSON

ISBN 978-91-89917-24-8| © Energiforsk April 2026

Energiforsk AB | Phone: 08-677 25 30 | E-mail: kontakt@energiforsk.se | www.energiforsk.se

Foreword

This report forms the results of a project performed within the Energiforsk Energiforsk Nuclear Power Concrete Program. The Program aims to increase the knowledge of aspects affecting safety, maintenance and development of concrete structures in the Nordic nuclear power plants. A part of this is to investigate possibilities to facilitate and simplify the work that is performed in the nuclear business.

Ensuring the integrity of reactor containment buildings is vital for nuclear power plant safety. Understanding potential weaknesses, such as gap formation between steel liners and concrete walls, is crucial to understand how the containment can be expected to behave in stressed circumstances.

This study investigates the causes and risks of gap formation in Nordic nuclear reactors, focusing on observed cases in Sweden. Through literature review, analytical calculations, and simulations, the project aims to clarify mechanisms and identify critical risk areas.

The results show that, in defect-free concrete, the risk of significant gap formation is low. Observed gaps are mainly linked to uneven shrinkage and drilling during decommissioning.

The study was carried out by Nils Janestad, Manouchehr Hassanzadeh, Camilo Rito Pi and Elin Torén Johansson, Sweco Sweden AB. The study was performed within the Energiforsk Nuclear Concrete Program, which is financed by Vattenfall, Uniper, Fortum, TVO, Skellefteå Kraft, Karlstads Energi, the Swedish Radiation Safety Authority and SKB.

These are the results and conclusions of a project, which is part of a research Program run by Energiforsk. The author/authors are responsible for the content.

Summary

The reactor containment building is the most important safety barrier in a nuclear power plant. It consists of a cylindrical, prestressed concrete structure with an embedded steel liner inside the containment wall to ensure integrity in the event of an internal accident. Nordic nuclear power plants have been decommissioned since the early 2000s. In recent years, openings have been made through the containment walls of decommissioned reactors, and gap formation between the steel liner and the inner concrete cylinder wall has been observed.

This study examines the risk and implications of gap formation in reactor containment buildings, as well as possible causes of the gaps observed in Swedish reactors. The work is based on a literature review, analytical calculations, and numerical simulations. It also identifies critical areas where gap formation is more likely and assesses whether gaps between the steel liner and concrete could negatively affect containment safety.

In Nordic reactors, the steel liner is typically embedded in the cylindrical wall between an inner concrete wall—primarily protecting the liner against internal missiles—and a thick outer load-bearing prestressed concrete wall with vertical and horizontal tendons.

The report investigates short- and long-term effects of creep, shrinkage, and climate variations in the inner and outer concrete cylinder walls separated by the steel liner. For defect-free concrete, the results indicate that long-term deformations from shrinkage and creep do not create a risk of gap formation between the outer concrete cylinder and the steel liner. For the inner concrete cylinder, gap formation due to shrinkage is shown to be possible but unlikely (or very small) in defect-free concrete, because the outer wall compresses the liner and inner wall. Overall, the study indicates that in a defect-free containment, gaps should not form in a way that affects the containment's ability to resist internal loads or perform its leak-tight function.

The report discusses potential explanations for the gaps observed in Swedish containment buildings after wall openings were made. The gaps are suggested to be linked to uneven shrinkage in the inner containment wall, which can induce bending when the wall is opened, in combination with the drilling method used.

Finally, the report proposes further research and measurement needs to better evaluate the risk of gap formation and its implications for structural integrity and liner corrosion.

Keywords

Gap formation, steel liner, reactor containment building, Nordic reactors, steel liner corrosion

Sammanfattning

Den viktigaste säkerhetsbarriären i ett kärnkraftverk är reaktorinneslutningsbyggnaden. Den utgörs av en cylindrisk förspänd betongkonstruktion med en ingjuten tätplåt i reaktorväggen, som ska säkerställa anläggningens täthet och integritet vid en olycka inifrån. Nordiska kärnkraftverk har avvecklats sedan början av 2000-talet. Under senare år har upptag genom reaktorinneslutningens vägg utförts, och i samband med detta har spaltbildning mellan tätplåten och den inre betongcylinderns vägg observerats.

I denna studie analyseras risker och konsekvenser av spaltbildning i en reaktorinneslutningsbyggnad, samt möjliga orsaker till de spalter som observerats i svenska reaktorer. Arbetet baseras på litteraturstudier, analytiska beräkningar och numeriska simuleringar. Vidare identifieras kritiska områden där spaltbildning kan förväntas uppstå, och det bedöms om spalter mellan tätplåt och betong kan påverka inneslutningens säkerhetsfunktion negativt.

I nordiska reaktorer är tätplåten i de flesta fall ingjuten i den cylindriska betongväggen. Denna består av en inre betongvägg, vars huvudsakliga funktion är att skydda tätplåten mot projektiler inifrån, samt en tjock, yttre lastbärande vägg av förspänd betong med vertikala och horisontella spännkablar.

Rapporten undersöker kort- och långtidseffekter av krypning, krympning och klimatvariationer i de inre och yttre betongcylinderväggarna, vilka separeras av tätplåten. Resultaten visar att långsiktiga deformationer från krympning och krypning i felfri betong inte medför risk för spaltbildning mellan den yttre betongcylindern och tätplåten. För den inre betongcylindern bedöms spaltbildning till följd av krympning vara möjlig men inte sannolik, alternativt mycket begränsad i felfri betong. Detta beror på att den yttre betongcylindern genom sitt tryck mot tätplåten även pressar den inre cylinderväggen. Sammantaget indikerar studien att spalter mellan tätplåt och betong inte bör uppstå i felfri konstruktion, och inte heller påverka inneslutningens förmåga att motstå interna laster eller upprätthålla täthet.

Rapporten diskuterar möjliga förklaringar till de spalter som observerats i svenska reaktorbyggnader efter att håltagningar har gjorts i väggarna. Spalterna bedöms kunna vara kopplade till ojämn krympning i den inre inneslutningsväggen, vilket kan inducera böjning när väggen öppnas, i kombination med den använda borrmetoden.

Slutligen föreslår rapporten att ytterligare forskning och mätningar behövs för att bättre kunna utvärdera risken för spaltbildning och dess konsekvenser för den strukturella integriteten och tätplåtens korrosion.

List of content

1 Introduction

The reactor containment building is the most important safety barrier at a nuclear power plant. It typically consists of a cylindrical, prestressed concrete structure with an embedded steel liner to ensure leak-tightness and integrity in the event of an internal accident. In Nordic reactors, the steel liner is in most cases embedded within the cylindrical containment wall between two concrete layers: an inner concrete wall, primarily intended to protect the liner from internal missiles and local impacts, and a thick, outer load-bearing wall of prestressed concrete with vertical and horizontal tendons. In an accident scenario, the steel liner is intended to act as the primary leak-tight barrier, separating the high-pressure containment atmosphere and radioactive substances from the external environment.

All Nordic reactors, except the newly constructed Finish rector Olkiluoto 3, have reached their intended service life and have entered long-term operation (LTO). In Sweden, as of 2026, four reactors have been decommissioned and are undergoing dismantling. To enable removal of internal components, holes have been drilled through the reactor containment wall. Following drilling, gaps were observed between the inner concrete wall and the steel liner.

The observed gap formation may be a consequence of detensioning of tendons and of the drilling and subsequent wall removal, and the underlying causes are not yet clear. It is considered likely that the gaps developed after drilling was completed, and that a defect-free containment wall would not exhibit such gaps. To assess whether gap formation is a problem for the safety of the reactor building, a conclusion needs to be drawn as to whether the gap formation originates from the drilling, or whether the gap formation was already present previously.

Previous projects within the Energiforsk concrete technology program for nuclear power have examined factors that increase the risk of steel liner corrosion. Gaps between the liner and concrete are a key contributor, since they can disrupt the passivation of the steel surface and thereby facilitate corrosion.

This work aims to identify the conditions and circumstances that increase the risk of gap formation, including locating zones within the containment where the likelihood of gaps is higher. By simulating both initial and long-term behavior of the containment wall and comparing results with observed gap locations, the study seeks to identify the main risks and mechanisms behind gap formation. For the case of observed gap formation in decommissioned reactors the question of whether the observed gaps may be attributed to the relaxation of cables during drilling is examined. The overall purpose is to provide a deeper understanding of the risk of gap formation in Nordic containments and its potential adverse effects on structural integrity.

1.1 BACKGROUND

Nordic nuclear power plants (NPPs) are located in Sweden and Finland, the only Nordic countries using nuclear power for electricity generation (as of 2025). The NPP fleet comprises two reactor types: boiling water reactors (BWRs) and pressurized water reactors (PWRs).

Both BWR and PWR units typically have in situ cast reactor containments with cylindrical concrete walls and a steel liner embedded within the wall section. The liner arrangement varies: in floors and roofs it is commonly cast into the slab or roof cupola; in some reactors it is instead placed directly on the inner concrete surface, making it directly exposed to the internal environment.

In Nordic containments, the steel liner is typically a 4–10 mm thick plate of high-grade steel. During construction it is cast or grouted against one or both sides, with inner and outer concrete surrounding the liner to achieve a continuous, leak-tight barrier. Liner tightness is verified through recurring pressure (leakage) tests performed throughout the containment service life. These tests also provide an opportunity to verify the structural response at a prescribed pressure level and detect potential changes in mechanical behavior; however, reliable verification requires displacement and strain measurements combined with theoretical analysis.

In recent years, dismantling of NPPs has revealed gap formation at multiple locations in containment walls. Understanding the mechanisms behind gap formation is necessary to assess its potential impact on structural integrity. Based on dismantling data, a literature survey, and analytical calculations, this report evaluates how different mechanisms may contribute to gap formation. Potential causes and risks are illustrated in Figure 1.

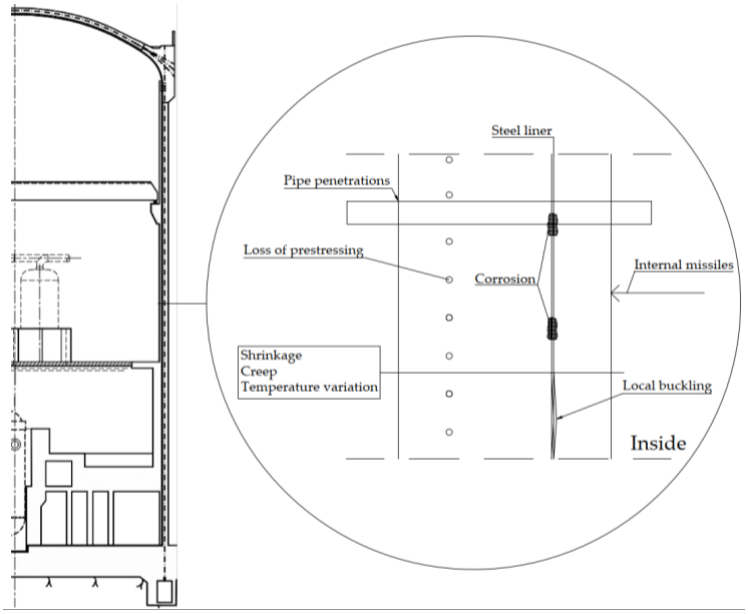

Figure 1. Illustration of a typical Nordic PWR containment building and the identified mechanisms of gap formation between steel liner and concrete (Roth et al., 2002).

1.2 PURPOSE AND SCOPE

The purpose of this project is to improve understanding of gap formation between the steel liner and the concrete in Nordic reactor containments. This is done by identifying possible causes and evaluating how gap formation may influence containment behavior and safety. The project also seeks to identify risk areas, conditions that increase the likelihood of gap formation, and any potential negative consequences associated with such gaps.

The scope of the study is to:

- Identify and evaluate observations of gap formation through a literature review, with a focus on Nordic NPPs.
- Identify possible causes of gap formation between the steel liner and concrete in containment walls.
- Simulate short- and long-term behavior of a representative reactor containment using analytical and numerical modelling, to study mechanisms that may lead to gap formation.
- Identify critical areas in containments where the risk of gap formation is elevated.
- Assess the effects of gap formation on the containment's structural behavior and safety functions.

1.3 METHODOLOGY

A major part of the project has focused on compiling and evaluating existing knowledge on steel-lined reactor containments and the mechanisms that may lead to gap formation. The work includes a literature review and a summary of reported cases of gaps between the steel liner and concrete in containment walls for Nordic reactors.

A case study was performed to assess short- and long-term behavior for a containment building represented by a generic Nordic reactor geometry. Analytical and numerical calculations were carried out to determine both initial and long-term effects from creep, shrinkage, and temperature variations in the cylindrical concrete containment wall. The results were compared with reported/observed gap formation to discuss possible causes, risk areas, expected effects, and the potential magnitude of gaps in the cylindrical wall.

The original plan included a site visit to a Nordic plant where gap formation had been observed, to perform measurements and assess site conditions. This could not be completed, and the project therefore relies on limited photographic documentation rather than measured field data.

It was also planned to use an existing detailed 3D FE model of a containment building. As this was not possible, a simplified 3D FE model of a typical Nordic containment wall was developed and used for the project's numerical analyses.

1.4 LIMITATIONS

For a Nordic NPP context, the study has focused on a generic containment wall geometry exposed to outdoor conditions, similar to Ringhals 2. This choice limits direct comparison with measured gap-formation data, but the impact is small because available field data on gap formation is very limited in any case. Due to the lack of measurements from decommissioned plants, the work therefore relies primarily on literature review and analytical/numerical simulation.

The inner and outer containment walls were originally designed as two separate concrete shells with a steel liner between, and are treated as separate walls in this project as well. The prestressing of the outer wall could influence contact pressure against the inner wall: tendon tensioning reduces the outer wall radius, which may compress the inner wall (via the liner which will be compressed as well), potentially increasing creep. Similar, internal pressure loads (e.g., pressure tests) may increase the pressure from the inner wall toward the outer wall, pressing the two walls together. Quantifying this interaction and its effect on inner-wall's stress state and deformations would require accurate measurements and more advanced coupled analyses and is therefore outside scope; the compression hypothesis would need dedicated measurement campaigns and further research to verify.

Analytical results based on Eurocode 2 creep and shrinkage models (CEN, 2014) have been compared with a simplified numerical model in which inner and outer walls are modelled separately. Use of existing detailed 3D FE models was not feasible due to ownership restrictions and time limits. Instead, the project developed a simplified model to study long-term response by applying creep and shrinkage as equivalent temperature loads. Several simplifications were adopted (e.g., no reinforcement modelling), but the model still provides an indication of the mechanisms and trends relevant to gap formation.

Finally, the influence of steel liner cut-outs/penetrations (pipes, manholes) and internal missile considerations is only addressed to a limited extent in the project.

2 Reactor containment buildings

Containment buildings in Sweden and Finland are associated with two reactor types: BWR and PWR, and the environmental exposure conditions differ between them.

In BWRs, the containment structure is entirely enclosed within the reactor building, so all external containment surfaces are governed by indoor environmental conditions, see Figure 2. In PWRs, the outer containment wall is exposed to the outdoor climate, see Figure 3, which introduces external temperature and moisture variations that can influence long-term behavior.

During operation, BWR containments are inerted with nitrogen, a practice generally not used in PWRs. Surface protection systems also differ: in BWRs, concrete surfaces in both the upper and lower drywell are typically treated with epoxy paint, while in PWRs the entire containment interior is commonly coated with paint forming a membrane (Sandberg, 2019).

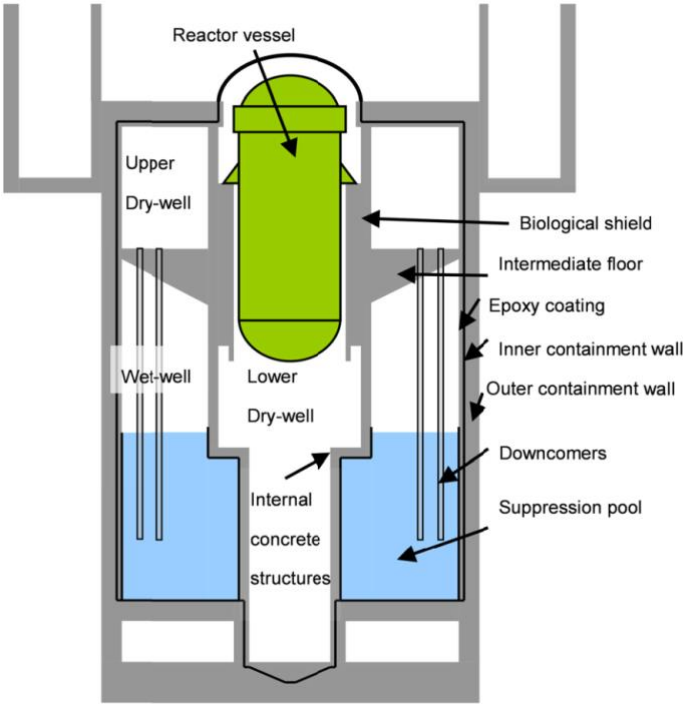

Figure 2. Schematic sketch of a BWR. Black line represents the steel liner and gray surfaces represents the concrete (Oxfall, 2016).

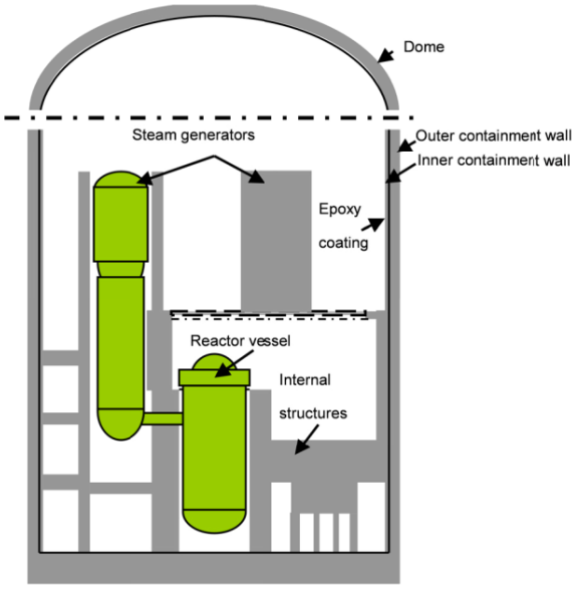

Figure 3. Schematic sketch of a PWR. Black line represents the steel liner and gray surfaces represents the concrete (Oxfall, 2016).

2.1 CONTAINMENT STRUCTURES IN SWEDISH AND FINNISH NUCLEAR POWER PLANTS

A reactor containment building is a key safety structure in a nuclear power plant, intended to prevent the release of radioactive material during accidents. Its cylindrical wall system typically comprises an outer reinforced concrete wall (often prestressed with horizontal and vertical tendons), an inner reinforced concrete wall, and a steel liner located between them. The liner improves resistance to internal overpressure, provides a gas-tight barrier to limit leakage of radioactive gases, and contributes to overall airtightness.

In BWR containments, the steel liner can be freely exposed in certain upper regions. In PWR containments with a spherical dome, the liner may also be freely exposed, see Figure 4 (e.g., Ringhals 3) illustrates a typical Nordic PWR configuration where the outer concrete surface is exposed to the outdoor environment.

Penetrations for pipes, manholes, and equipment are formed by recesses in the steel liner. For larger recesses, shear connectors are used to ensure composite action and transfer forces between liner and concrete.

Containment buildings are designed to withstand extreme external loads such as earthquakes and floods, maintaining structural stability and leak-tightness. They also incorporate filtered venting or gas handling systems to manage any releases during an incident. Because performance depends on the integrity of both the concrete and liner—including the development of cracks or gaps—regular inspection and maintenance are essential. In a severe accident, the containment functions as the final engineered barrier protecting the public from radiation exposure.

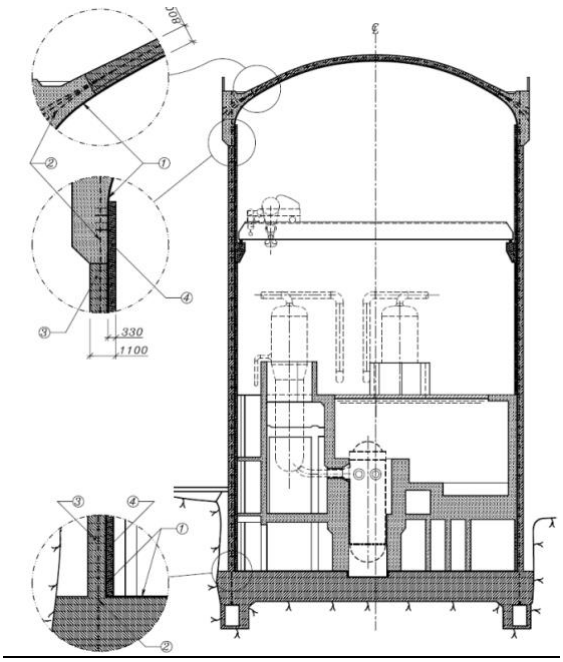

Figure 4. Section through Ringhals III illustrating the steel liner placement within the reactor containment building. The number 1 is the steel liner (Sandberg, 2019).

Swedish and Finnish containment walls were constructed using different approaches depending on reactor type and construction period. Based on available data for Nordic NPPs, the cylindrical containment wall geometries vary between plants. Reported internal diameters range from 9.3 m (Oskarshamn 1) to 35.4 m (Ringhals 2–4).

The combined thickness of the inner wall, steel liner, and outer wall is commonly about 1.1 m, typically consisting of an inner missile protection wall of roughly 0.3 m and an outer containment wall of about 0.8 m. The height of the concrete containment cylinder varies with containment concept and reactor type, reaching up to approximately 59 m (Ringhals 2). The steel liner is generally fabricated from 5–10 mm thick steel plates; in some plants the liner is thicker in the lower parts of the containment. Liner joints are commonly executed as butt welds with a back weld (Roth et.al., 2002), (Barslivo et al., 2003).

2.1.1 Construction of the cylindrical containment wall

Cylindrical containment walls in Swedish and Finnish nuclear power plants follow the same overall design principle: a thick outer load-bearing concrete wall, a steel liner on the inside to ensure leak-tightness, and an inner concrete wall protecting the liner. While this construction concept is common to Nordic reactors, the execution differs between plants, primarily in terms of casting sequence and steel liner assembly.

These alternative construction methods are schematically illustrated in Figure 5, showing differences in (i) the casting stages of the inner and outer cylindrical walls and (ii) how the steel liner has been counter-cast. In some cases, concrete is cast against the steel liner on both sides, so the liner effectively acts as formwork. In

other cases, concrete is cast against the liner on only one side, while the opposite side is completed by grouting (injection) between the liner and the concrete.

The chosen construction stages influence early-age drying and shrinkage as well as long-term moisture and deformation development. This must therefore be considered when assessing gap formation in cylindrical containment walls in reactor containment buildings.

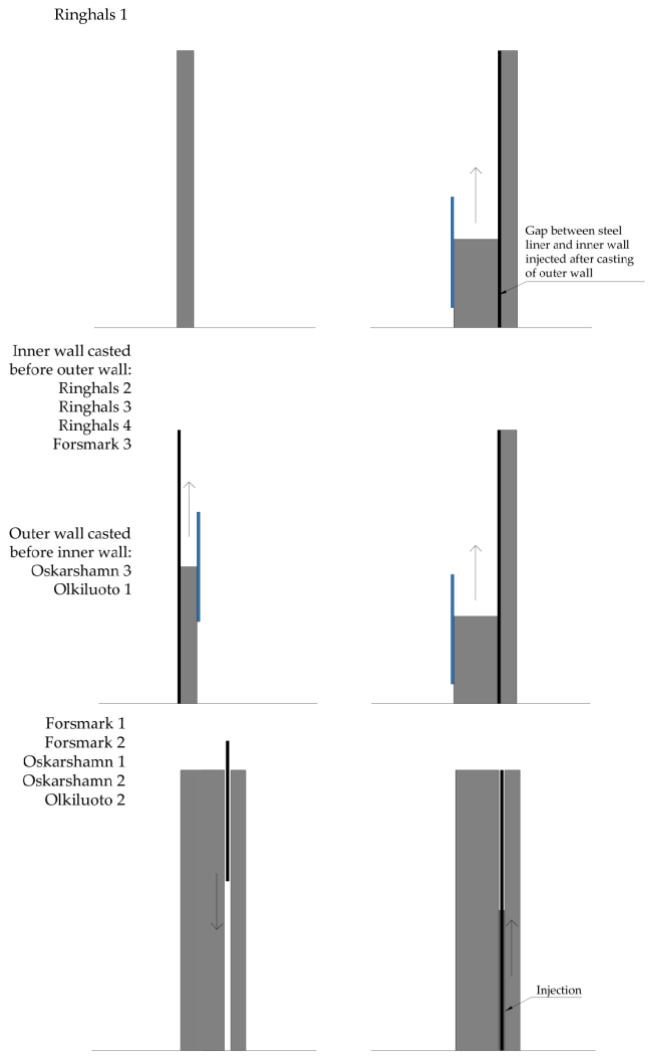

Figure 5. Techniques for casting and injection against steel liner in Swedish and Finnish nuclear power plants, reproduced from (Sandberg, 2019).

Techniques for casting and injection against steel liners in Swedish and Finnish reactors are further presented by Sandberg (2019), who summarizes three main casting procedures:

- **Ringhals 1:** The inner wall was cast using the slipform method. The steel liner at the top of the cylindrical wall was then manufactured and successively lowered. The liner was installed on the outside and fitted with attachments for recesses, reinforcement, etc. Once the steel liner shell was completed, the outer load-bearing part of the containment cylinder was cast. The gap between the inner concrete cylinder and the steel liner was then injected (grouted).

- **Ringhals 2–4, Forsmark 3, Oskarshamn 3, and Olkiluoto 1:** The steel liner was first manufactured in its entirety, after which the inner and outer concrete cylinders were produced using slipform casting. Penetrations and recesses were mounted on the steel liner. In Oskarshamn 3 and Olkiluoto 1, the outer wall was cast first; in the other plants, the inner wall was cast before the outer wall.

- **Forsmark 1–2, Oskarshamn 1–2, and Olkiluoto 2:** Both inner and outer walls were cast using slipform techniques, and the steel liner was lowered into the 0.10–0.12 m wide gap. The liner was manufactured at the top by progressively welding plates. Penetrations were formed by inserting recesses during slipform casting. The space between the cast concrete and the steel liner was then injected (grouted).

2.2 CLIMATE AND ENVIROMENTAL CONDITIONS

Climatic conditions in Swedish and Finnish reactor containments vary seasonally for PWRs, since the outer containment wall is exposed to the surrounding climate. In a BWR containment, the internal climate is largely unaffected by the external climate, and changes mainly depend on operational conditions. During reactor operation, temperatures inside the containment are elevated relative to the outside; within the containment, temperature generally increases with elevation because higher levels are closer to the reactor core, where heat production is greatest. During shutdown, the temperature is approximately uniform across all levels, since there is no active reaction in the reactor core (Sandberg, 2019).

To evaluate creep and shrinkage effects in the inner and outer containment wall, average temperature and humidity values for a representative wall section are used. Initially, after demolding, the concrete is assumed to be in equilibrium at 100% relative humidity (RH). As drying shrinkage progresses, the concrete primarily dries towards the outer surface, since moisture transport towards the steel liner is very slow.

An assessment of RH development in inner and outer containment walls in Nordic NPPs is presented by Oxfall (Oxfall, 2017). The study concludes that drying of containment walls is very slow; even after many years, RH remains high. Temperature and moisture variations in Nordic PWR containment walls reported by Oxfall are interpreted for low and high elevations to obtain average through-wall values, shown in Figure 6. These average values are used in the evaluation of initial and long-term effects.

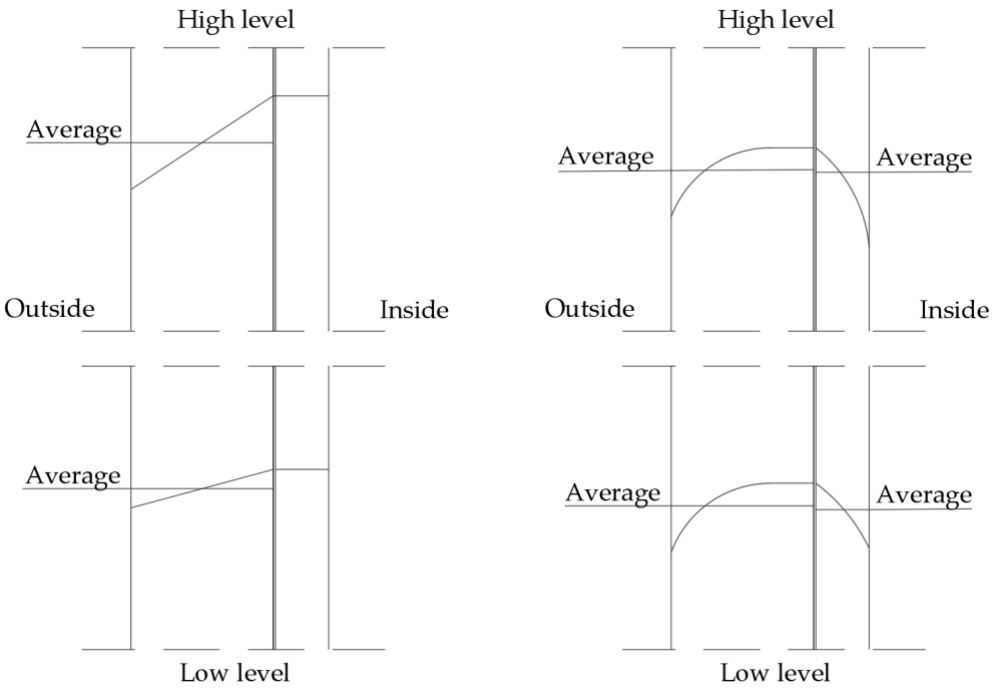

Figure 6. Left: Average temperature variation for a Nordic PWR. Right: Average variation in relative humidity (RH) for a Nordic PWR. Based on Oxfall (2016).

2.2.1 Temperature conditions BWR reactors

For BWRs, moisture emitted from the concrete and pools is absorbed by the air inside the containment. To avoid impacts on sensitive equipment, the air is dehumidified during operation. During operation, the internal temperature is slightly above 20 °C at lower elevations and increases to about 50–60 °C at higher elevations. During shutdown, no significant temperature gradient develops across the containment wall, and the temperature is slightly above 20 °C on both sides of the wall (Oxfall, 2016). These temperature conditions are shown schematically in Figure 7.

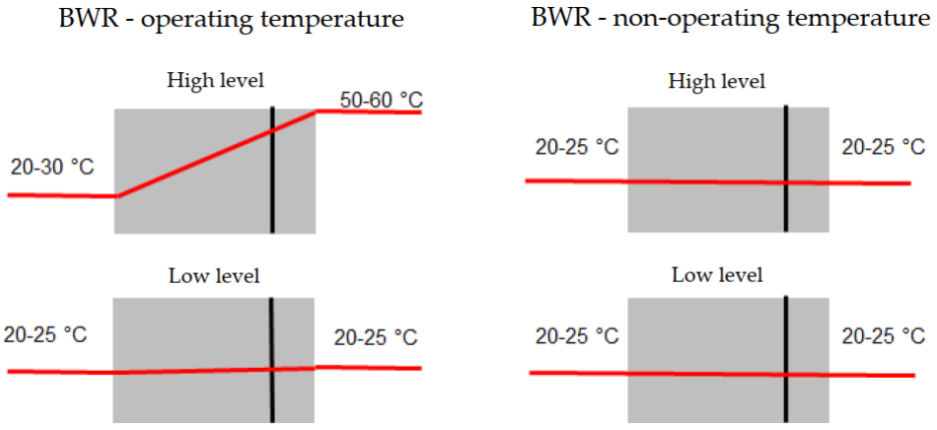

Figure 7. Temperature variations in the cylinder wall of BWR reactors (Sandberg, 2019).

2.2.2 Temperature conditions PWR

For PWRs, the containment wall is subject to significant temperature gradients. The exterior temperature follows the outdoor climate, while the interior temperature during operation typically ranges from 20–30 °C at lower elevations and increases to around 40 °C at higher elevations. During shutdown, the internal temperature is approximately 20 °C. These temperature conditions are illustrated schematically in Figure 8.

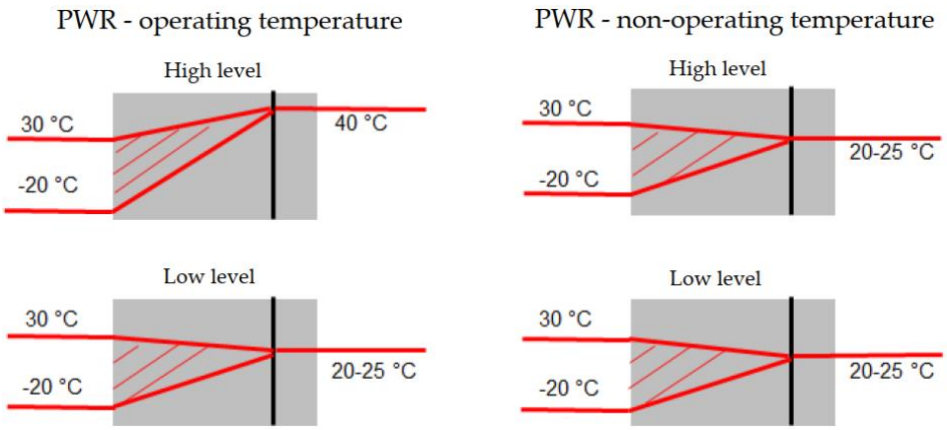

Figure 8. Temperature variations in the cylinder wall of PWR (Sandberg, 2019).

2.2.3 Temperature conditions for case study

As previously described, the case study adopts the geometry of a generalized Nordic reactor building. To evaluate temperature variations, Ringhals—located on Sweden's west coast near Varberg—has been selected as the reference site. Yearly outdoor temperature data for the Ringhals and Varberg weather stations are presented in Table 1.

The data were obtained from SMHI (the Swedish Meteorological and Hydrological Institute) and compiled as mean annual temperatures from 1975 to 2025 (a 50-year period), sorted by mean annual temperature. The dataset is used to represent a reference mean temperature one year after construction, with construction assumed to start in 1975, and the mean temperature 50 years after construction. Two different weather stations are included due to the lack of continuous long-term data from a single station.

Table 1. Data collected from SMHI (smhi.se) and represent mean annual temperatures for the period 1975-2025 (SMHI, 2025).

Location	Mean temperature year 1975 [°C]	Mean temperature 1975-2025 [°C]
Ringhals, Bua Sweden	8,6	
Varberg Sweden		8,0

2.2.4 Moisture conditions BWR and PWR

The vapor content is assumed to follow the external conditions surrounding the containment. For BWRs, this implies that the vapor content at the containment wall corresponds to that in the reactor building enclosing the containment. For PWRs, the outdoor climate governs, resulting in low relative humidity (RH) at higher elevations on the containment wall and significantly higher RH at lower elevations.

Analyses of both the interior and exterior surfaces of the cylindrical wall indicate that RH increases with depth and remains high (about 80–85%) closest to the steel liner, even after many years of service life (Oxfall, 2016). Based on these findings, relative humidity profiles are established and presented in Figure 9.

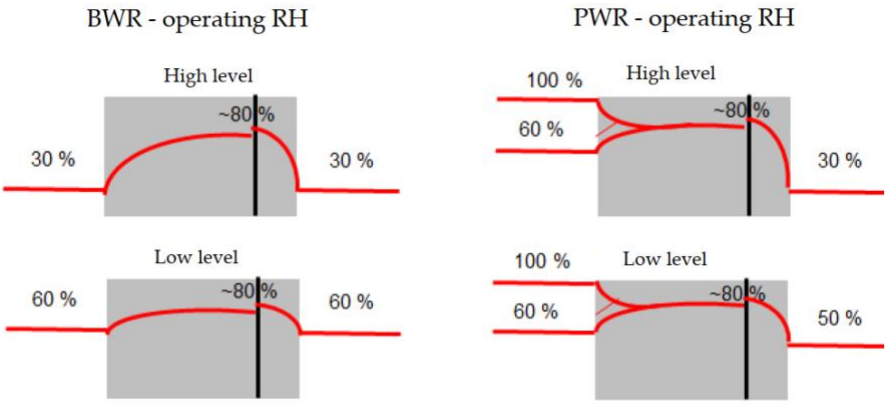

Figure 9. Relative humidity in the cylindrical wall and the surrounding spaces in BWR and PWR during operation (Sandberg et.al., 2019).

2.2.5 Moisture conditions for case study

As for the mean temperature, moisture variations at the Ringhals site near Varberg are evaluated for the case study. These RH values are used to calculate the final creep and shrinkage in the case study.

The outer containment wall dries outward towards the surrounding environment. The annual average outdoor RH at Ringhals is assumed to be 80%, based on data from SMHI.

For the inner containment wall, exact information on the mean RH inside the containment is not known to the project. Therefore, assumptions are made based on RH profiles presented in Figure 9. Since the inner concrete surface is treated

with an epoxy layer, drying of the inner reactor wall is expected to occur very slowly. As indicated by the measurements, even after a long period (50 years) the RH within the inner concrete wall remains high. It is therefore assumed that the long-term average RH of the inside is 70%, which is a simplifying assumption adopted for the calculations.

2.2.6 Timeline of construction

To evaluate both short- and long-term effects in the case study, a construction timeline is defined. Since construction stages and building procedures differ between reactor types, a generalized timeline for containment construction is established, see Figure 10, to consistently account for short-term and long-term material behavior (e.g., early-age effects versus long-term creep/shrinkage).

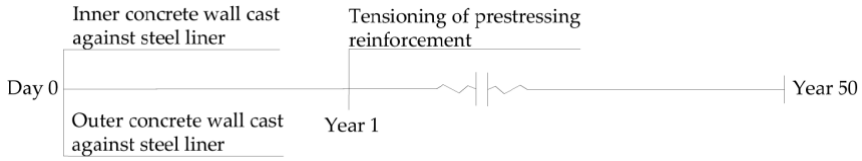

Figure 10. Visualized general timeline of construction of a containment building for the case study.

The cylindrical outer wall of a containment building is prestressed in both the horizontal and vertical directions. The time at which the tendons are prestressed varies with the construction sequence and whether the tendons are grouted.

In this case study, the prestressing time is assumed to be 1 year after casting of the containment walls. As a simplification, the inner and outer walls are assumed to be cast simultaneously. The rationale for assuming prestressing after 1 year is that the initial creep and shrinkage effects are largely completed by then, so the analysis can focus on long-term effects.

2.3 OBSERVATIONS ON GAP FORMATION IN SWEDISH REACTORS

When replacing large internal reactor components or during reactor dismantling, openings may need to be cut through the containment wall to enable material transport. Creating such openings typically requires detensioning (releasing) vertical and horizontal tendons around the intended opening.

For the four Swedish reactors recently taken out of service, collected site data show that during the hole-making process, gaps formed between the inner concrete wall and the steel liner in all cases studied. Whether this gap formation is primarily driven by the demolition/opening procedure itself or by other contributing factors remains unresolved.

For Ringhals, the observed gap formation is documented in detail for each reactor. For Ringhals 2, finite element calculations performed in connection with the 1989 steam generator replacement are also included for comparison.
Observed/estimated gap formation data between the steel liner and the concrete are presented in Table 2. Note that the listed gap values are site estimates and were not obtained through precise instrumented measurements.

Table 2. Observed gap formation data for the Ringhals containment buildings were provided by Vattenfall. Note that the reported gap values are site estimates and were not obtained using precise instrumented measurements.

Construction part	Observation	Gap formation
Opening between containment and fuel building at Ringhals 2 in 1989.	Estimated gap formation from FE-calculations made between inner concrete cylinder wall and steel liner.	2 mm
	Gap formation between inner concrete cylinder wall and steel liner.	1-2 mm
Demolition and dismantling of Ringhals 2. Opening between containment and fuel building.	Gap formation between inner concrete cylinder wall and steel liner.	Ca 2-5 mm
Steam generator exchange Ringhals 3. Opening of containment wall.	Gap formation between inner concrete cylinder wall and steel liner.	1-2 mm
Steam generator exchange Ringhals 4. Opening of containment wall.	Gap formation between inner concrete cylinder wall and steel liner.	2-3 mm

2.3.1 Gap formation observation Ringhals 2 – Generator replacement in 1989

During the steam generator replacement at Ringhals 2 in 1989, an opening was made in the reactor containment wall to allow material transport. Prior to cutting the opening, finite element (FE) analyses were performed to evaluate the effect of tendon detensioning and hole-making on concrete wall deformations. The calculated vertical and radial deformations were later compared with measured values; the calculation results are shown in Figure 11.

The opening was created by releasing 8 vertical tendons, 18 horizontal tendons across the opening, and 9 tendons located above and below the opening. In the FE model, two perpendicular symmetry planes were used, so only one quarter of the cylindrical containment (including the opening) was analyzed.

Measured gap data after opening the containment wall (Table 2) indicate a gap of about 1–2 mm. This matches well with the calculated radial deformation of approximately 2 mm, see Figure 11. The agreement suggests that the gap observed in 1989 was most likely caused by detensioning of the tendons around the opening, and that the gap was not present prior to tendon release. The calculations further indicate that re-tensioning reduces the radial deformation compared with the detensioned condition (and even relative to the initial state), implying that any gap around the opening should close after re-tensioning.

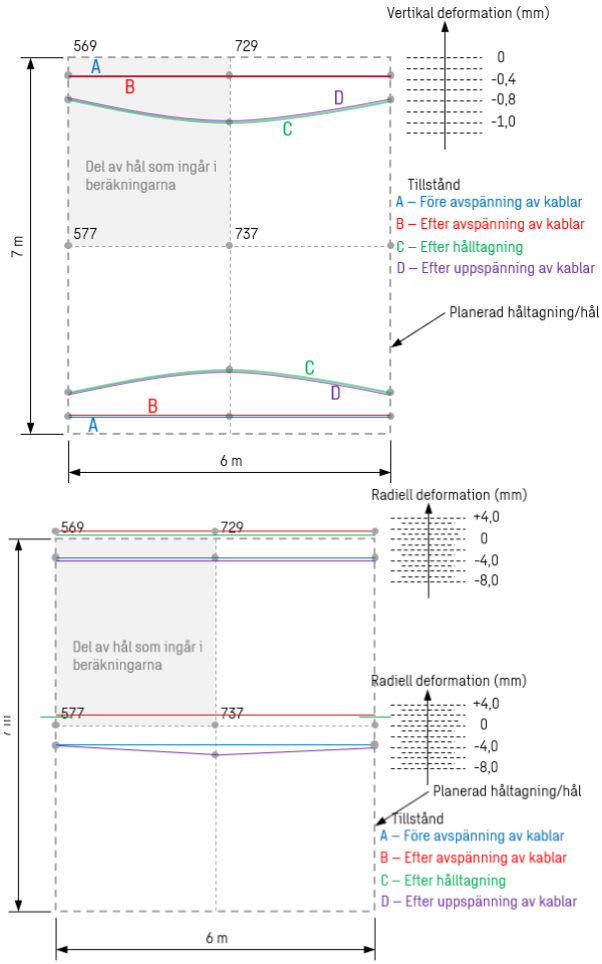

Figure 11. Vertical and radial deformation analysis performed before steam generator replacement in 1989. Figures reconstructed from data given in calculations of steam generator exchange Ringhals 2 in 1986 (Carlsson et.al., 1986).

2.3.2 Gap formation observation Ringhals 2 - Dismantling

In connection with dismantling and demolition at Ringhals 2, an opening was created between the reactor containment and the fuel building, close to the opening made during the 1989 steam generator replacement, see Figure 12. This provided an opportunity to monitor the reactor building's structural response during de-tensioning of the horizontal and vertical tendons around and above the wall opening. Sensors were installed to measure changes in strain and deformation, as well as temperature, throughout the de-tensioning period.

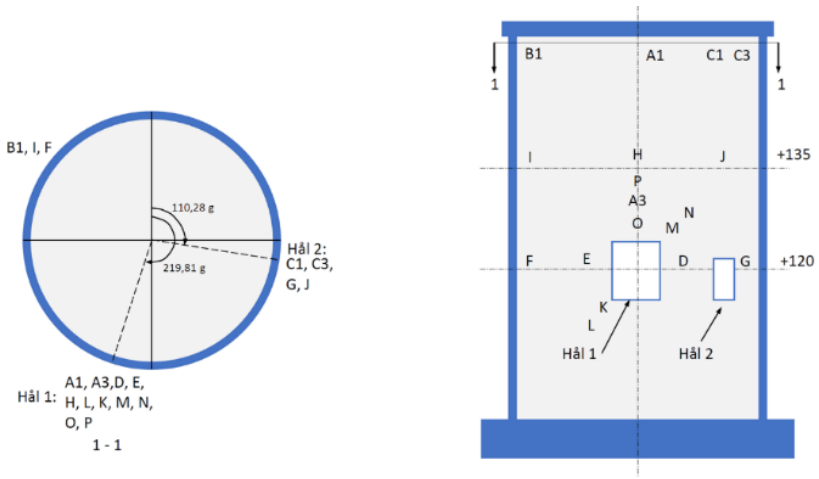

Figure 12. Location of opening 1 (steam generator exchange in 1989), and opening 2 (Ringhals 2 dismantling).

An independent Energiforsk report presents the monitoring results and is planned for publication in 2026. Parts of the data from that work have been made available and are included in the present report.

The report evaluates the 2023 creation of an opening in the Ringhals 2 containment wall and the associated de-tensioning program, in which 23 vertical and 97 horizontal tendons were de-tensioned between 2023-08-22 and 2023-12-20. During this period, temperature variations affected the measurements. Total strain and deformation were therefore interpreted by assessing whether the recorded values followed the expected temperature-driven response.

For a structure that is essentially stress-free and not subject to restraints or temperature gradients, sensor readings should largely track seasonal temperature variations: measured strains would typically decrease from September towards February and then increase again towards September. In this case, the measured strain variations did not fully correspond to the temperature changes. The results of this report can in the future be used to support further investigation of the observed gap formation, by providing measured strain/deformation trends during tendon de-tensioning and their relationship to temperature. The average horizontal strain measured during detensioning of all tendons is approximately 200–400 microstrain.

As in the pre-1989 case, gap formation was observed after 2023 opening of the containment wall. Gaps were found around the opening through the containment and fuel building towards the inner containment wall and steel liner, see Figure 13.

The larger gap formation observed after cutting an opening in the reactor containment - compared with the results of the theoretical analysis in 1989 may be due to one or more of the following reasons: (i) a second tensioning event, (ii) a longer time between tensioning and hole creation, (iii) the facility being in a cold state for an extended period, and/or (iv) effects from drilling through the wall. These are plausible causes that should be verified.

a)

b)

Figure 13. Gap formation observation at Ringhals 2 (2023). (a) Containment wall with the inner wall located on the left side. (b) Containment wall with inner wall located at the top. (Photos provided by Vattenfall).

Notably, the gap formation occurs between the inner concrete cylindrical wall and the steel liner. During construction of the Ringhals containments where gap formation has been observed, the walls were cast against the steel liner for both the inner and outer containment wall. Long-term effects of creep and shrinkage may influence the concrete and thus the steel–concrete interface adhesion; this is investigated in the report. However, it is likely that the wall opening itself contributes to the observed gap formation. Two hypotheses are therefore presented and will be further investigated in the report.

Hypothesis 1 – shrinkage-induced stress gradient and local wall bending near the opening

The gap may originate from drying shrinkage, where the inner concrete surface shrinks more than the surface facing the steel liner, creating a shrinkage-stress gradient through the wall thickness. In a continuous (unperforated) cylinder, the concrete is restrained from local "buckling-type" deformations. When a section of the wall is opened, the local stiffness is reduced around the opening boundary. Existing stresses within the wall section may then cause the concrete to bend towards the inner surface, creating a small gap between the steel liner and the inner concrete wall. See Figure 14 for illustration of hypothesis 1. This hypothesis is discussed further in the report.

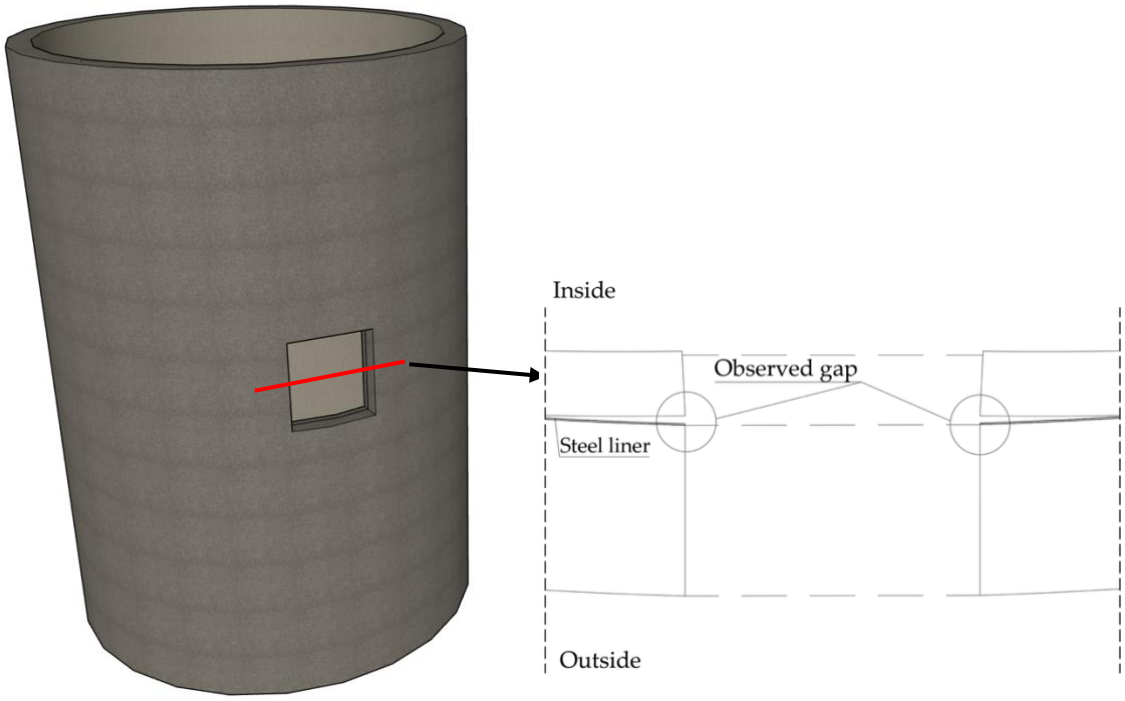

a) b)

Figure 14. Schematic illustrations used to exemplify Hypothesis 1. (a) Wall opening in a reactor containment building. (b) Wall section from the cut-out hole with shrinkage-induced stress gradient and local bending near the opening. The illustrations are conceptual and does not include the roof cupola or the floor base.

Hypothesis 2 – effects from the hole-making process (demolition/drilling/coring)

The hole-making procedure may contribute to the observed gap formation between the steel liner and the concrete. When creating an opening in a reactor wall, concrete cores are typically drilled around the opening after the post-tensioning cables have been de-tensioned. The drilling method—and the side from which drilling is performed—can influence the formation of gaps around the hole.

If the opening in the inner reactor wall is removed first, and drilling is then performed from the outside through the outer wall, this sequence may affect the size of the resulting gap. The drilling procedure can be described as:

1. The opening in the inner reactor wall is drilled from the inside.
2. The inner wall core is removed.
3. Drilling is then performed from the outside, through the outer wall, until the drill reaches the steel liner.

In this case, when the drill reaches the steel liner from the outside, it may push against the edge of the opening in the inner wall, widening any existing gap. The bond between the steel liner and the concrete is sensitive to vibration and heat generation and is not expected to remain intact between the surfaces around the opening. Assuming the liner plate is elastic, it should spring back toward its original position, leaving a residual gap between the inner concrete wall and the steel liner, see Figure 15 for illustration of hypothesis 2. Whether and to what extent this hypothesis can explain the observed gap formation is discussed further in the report.

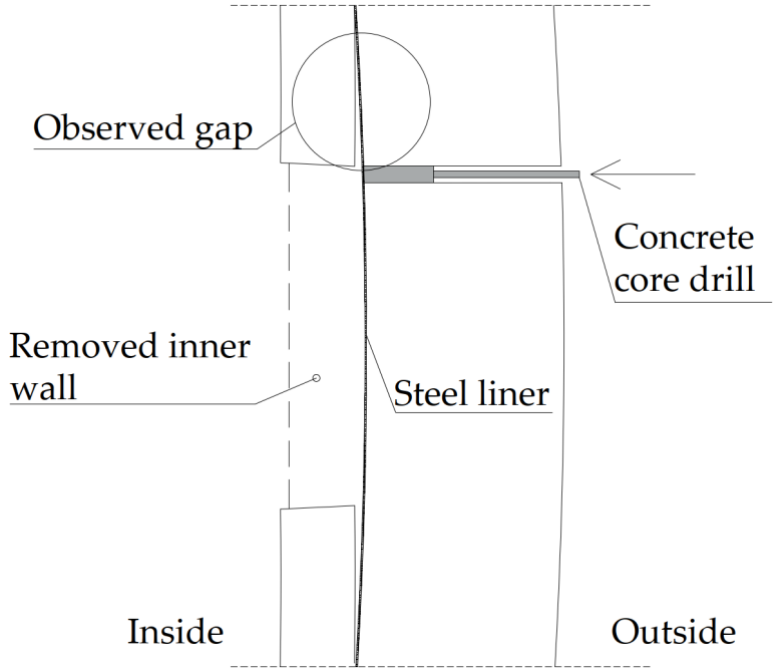

Figure 15. Illustration of the wall hole creation and the effect of drilling according to Hypothesis 2.

2.3.3 Gap formation observation Ringhals 3 – Generator replacement

During the inspection after the opening was created for the steam generator replacement at Ringhals 3, delamination between the steel liner and the inner concrete wall was measured at 1–2 mm. An analysis was performed to investigate the gap formation. The conclusion was that the measured gap would be compressed again during re-tensioning of the tendons, with possible local residual deviations at discontinuities such as lifting lugs on the steel liner. Similar behavior was also reported during creation of the opening for the steam generator replacement at Ringhals 2. Unfortunately, no photographs are available documenting the measured gap formation during the steam generator replacements.

2.3.4 Gap formation observation Ringhals 4 – Generator replacement

As at Ringhals 3, gap formation was observed at Ringhals 4 after the opening was created for the steam generator replacement. A gap of approximately 2–3 mm was observed between the inner concrete wall and the steel liner. Photographs from the generator replacement cannot be included in this report due to restrictions, but they indicate that drilling was performed from both sides, after which the steel liner was cut.

Figure 16 presents a schematic illustration of gap formation observed in Swedish containment buildings during opening of the reactor wall. The illustration is based on a generic containment wall similar to that of Ringhals 4. The observed gap is shown on the left-hand side of the steel liner, facing the inner wall, as a small separation between the steel liner and the concrete.

Figure 16. Schematic illustration of gap formation observed in Swedish containment walls during opening of the reactor wall. The inner containment wall is shown on the left-hand side, where a gap is present between the steel liner and the inner concrete wall.

2.4 PREVIOUS RELATED STUDIES

A substantial amount of work has been carried out within the framework of the Energiforsk Concrete Program Nuclear Power, among others. Results from selected previous projects relevant to gap formation are summarized to provide insight into the behavior of reactor containment buildings and the potential risk of gap formation.

2.4.1 Radial displacement of containment building over time and pressure test

In the Energiforsk project on instrumentation and modelling of a reactor containment building (Gasch et al., 2018), radial displacement and hoop strains were analyzed using both a three-dimensional finite element ring model and an axisymmetric model. The project evaluated a proposed instrumentation system for the BWR reactor containment at the Finnish nuclear power plant Olkiluoto 2, see Figure 17, to measure global and local structural deformations as well as moisture and temperature conditions. In the modelling, drying shrinkage was neglected by assuming $\varepsilon_{cd} = 0$, justified by a moisture-tight epoxy barrier on both sides of the containment wall.

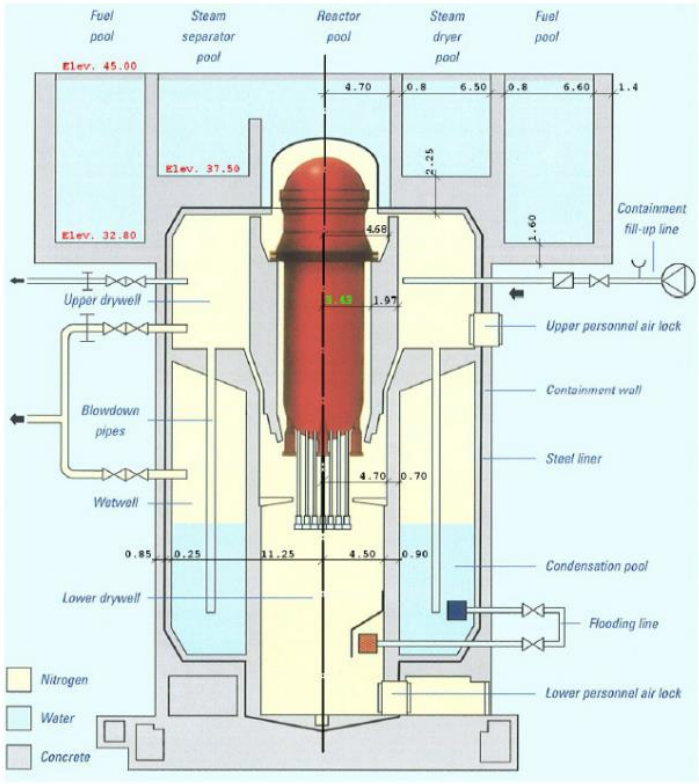

Figure 17. The overall geometry of Olkiluoto 2 including main dimensions (Teollisuuden Voima Oy, 2008).

The project investigated a sequence of analysis steps to assess the effect of a pressure test. The results are presented for six stages: (1) self-weight application, (2) autogenous shrinkage, (3) tendon activation, (4) 35 years in service including creep, shrinkage and tendon relaxation, (5) application of the temperature field, and (6) an internal pressure test of 3 bar acting on the containment structure.

The results are presented in Figure 18, which shows the radial displacement for the ring model, and Figure 19, which shows the microstrain. The strain is initially low because shrinkage is assumed to occur mainly during the first year and drying shrinkage is not included. By stage 4, when long-term effects and tendon behavior are accounted for, the radial displacement is approximately −2 to −3 mm, depending on the height considered. When the internal pressure test is applied in stage 6, the radial displacement increases due to pressurization.

The simplified numerical analyses showed good agreement with the measured radial response from the conducted pressure test. The results indicate that, for a defect-free containment with no loss of tendon force, the outer wall displacement decreases over time and therefore a gap is unlikely to form between the embedded steel liner and the concrete. The largest displacement occurs around mid-height of the containment structure, likely because this region is least restrained, being farthest from the boundary conditions imposed by the roof and floor slab.

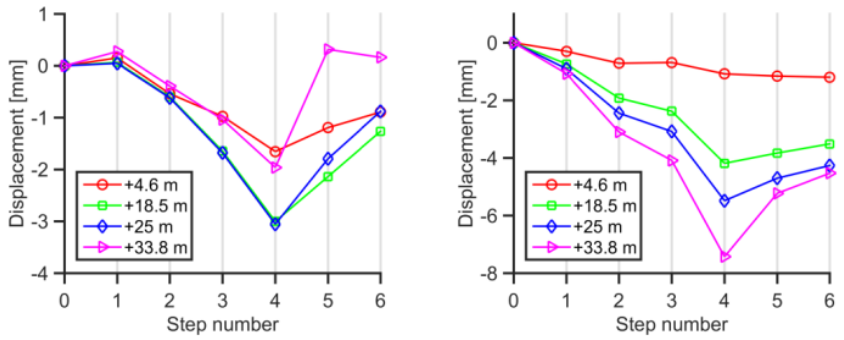

a) b)

Figure 18. Radial displacement (a) and vertical displacement (b) at three different heights of the containment wall. Values are plotted at the end of each analysis step (Gasch et.al., 2018).

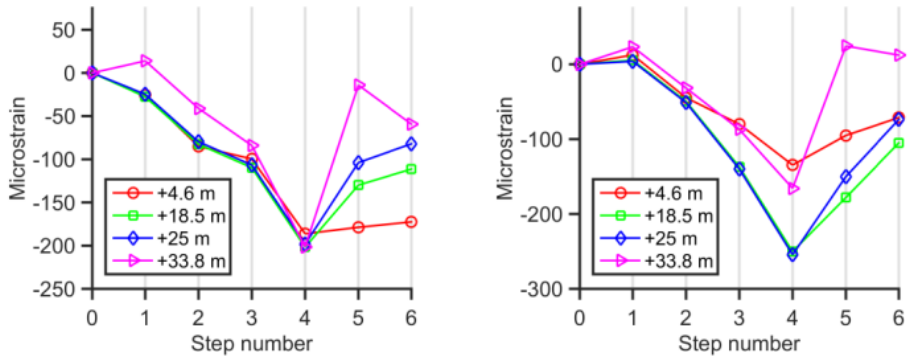

a) b)

Figure 19. Vertical (a) and hoop strain (b) on the outer surface of the containment wall at three different heights.

Values are plotted at the end of each analysis step and represent the total strain (Gasch et.al., 2018).

2.4.2 Radial deformation in case of loss in tendon force

In Reaktorinneslutningarnas respons vid höga inre tryck och reducerad förspänning (Hassanzadeh et al., 2018), internal pressure tests were simulated using FE models to study containment response under reduced prestressing, representing tendon breakage, damage, or release. The study is based on a Swedish PWR-type containment and includes both a ring model and a global 3D model; the case study concerns an outer wall with injected (grouted) tendons. Load cases were defined to represent local loss of tendon capacity, enabling assessment of the resulting radial displacement—which is directly relevant when evaluating potential gap formation and its implications for liner–concrete interaction.

Results from the ring model indicate that if damage occurs during a pressure test such that the load-bearing capacity of horizontal tendons is completely lost over a local segment, permanent (residual) radial deformation develops mainly in the damaged region. For loss over approximately 3 m, the residual deformation in the damaged area is about 3 mm; for loss over approximately 14 m, it increases to about 6 mm, see Figure 20. The simulations also show that the deformation remains relatively localized: in undamaged parts of the containment, the maximum residual deformation is approximately 1 mm and 4 mm for the 3 m and 14 m cases, respectively. Vertical deformation caused by loss of force in horizontal and/or vertical tendons is reported to be significantly smaller than the radial deformation.

Comparing the intact, tensioned condition with the reduced-prestress cases, both the ring model and the global 3D model show that the relative radial deformation during a standard pressure load test is on the order of 5 mm in the wall field middle (mid-height between two counterforts), when referenced to the condition where the enclosure is fully prestressed.

For containments such permanent radial deformations may be relevant in the context of gap formation, since radial opening at the liner–concrete interface can reduce composite action and potentially affect liner boundary conditions and local stress/strain demands. The deformation magnitudes reported by Hassanzadeh et al. (2018) are also consistent with measured gap formation presented in Chapter 2.3, where gaps have been observed in areas where tendons have been released, with values comparable to those indicated in Figure 20.

a)

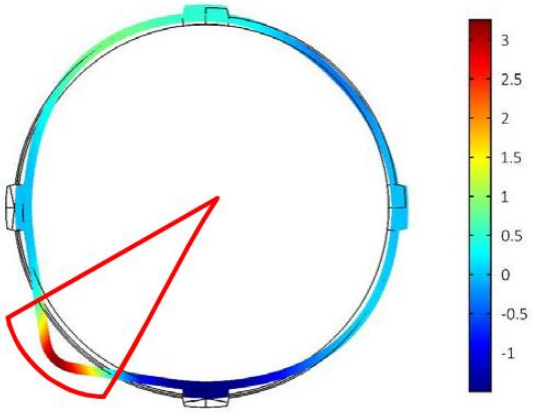

b)

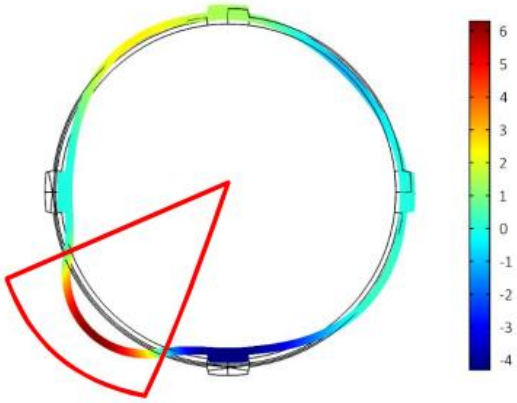

Figure 20. (a) Residual radial deformation (mm) for the case where the horizontal tendon force is completely absent over a 3 m segment in the mid-field region. (b) Residual radial deformation (mm) for the case where the horizontal tendon force is completely absent over a 14 m segment in the mid-field region (Hassanzadeh et al., 2018).

3 Mechanisms for gap formation between steel liner and concrete

Gap formation may result from a range of deterioration and/or construction-related processes. Although nuclear containments are designed for extreme load cases, the most frequent load effects in service are typically associated with restrained temperature variations. This action alone is not usually critical; however, the structural response is also influenced by creep, shrinkage, and relaxation of prestressing tendons, which may generate restraint forces that create conditions conducive to gap formation (Roth et al., 2002).

Steel embedded in concrete is normally in a passive state due to the highly alkaline pore solution and therefore does not corrode. Passivity may be lost if the pH decreases below approximately 9.2 (e.g., as a result of carbonation) or if the chloride content at the steel surface exceeds the critical chloride threshold. In a reactor containment, neither of these conditions is considered credible: carbonation requires sustained CO_2 ingress over time, which is limited for the containment walls, and there is no expected persistent chloride source that would lead to chloride accumulation in the concrete.

If the steel is not in contact with the concrete (e.g., due to a liner–concrete gap or a void), it is no longer protected by the alkaline environment and is not passivated; in the presence of moisture and oxygen, this may lead to corrosion. If corrosion occurs, the corrosion products (rust) typically occupy a larger volume than the original steel, which can generate local expansive forces and may contribute to the formation or further widening of a gap at the liner-concrete interface.

An Energiforsk review of potential corrosion risks for cast-in steel liners concludes that corrosion can develop on the liner surface if a partially air-filled cavity exists. For corrosion to become severe- leading to a larger gap and a meaningful reduction of liner cross-section-both a sufficiently large cavity and the presence of heterogeneities or foreign objects that accelerate the process are generally required (Sandberg et al., 2019).

Another Energiforsk study focusing on air transport through containment structures notes that corrosion of cast-in liners may be initiated by carbonation and/or chlorides. Corrosion can in turn promote gap formation because the expansion of corrosion products increases the effective volume at the steel–concrete interface. However, due to the large wall thicknesses in containments, carbonation and chloride ingress are typically too slow to reach the liner within a reactor's design life—unless air and moisture are transported through defects such as large cracks or voids (Malm et al., 2021).

Steel liner cut-outs are required for penetrations such as pipes and manholes. These regions are more susceptible to reduced composite interaction between liner and concrete due to geometric discontinuities and material transitions. In addition, prestressing tendons in the outer wall are commonly routed around penetrations, altering the local stress field around openings and potentially contributing to gap formation and, in some cases, reduced structural capacity. Shear connectors are

often used to improve interaction and reduce the likelihood of gaps developing at the liner interface.

To assess the severity and implications of a gap—and to identify critical locations—both the causes of gap formation and its effects on structural integrity need to be established. Chapter 2.3.2 presents and further discusses two hypotheses regarding observed gaps in Swedish reactors at wall penetrations. The following conditions are evaluated:

- Corrosion processes
- Restraint forces from environmental and material effects
- Geometric changes in the wall, such as liner cut-outs for pipes and manholes

3.1 CORROSION-RELATED MECHANISMS

A key difference between a steel liner and conventional steel reinforcement is the liner's large, continuous surface area and its reliance on a robust steel–concrete interface for structural performance and corrosion protection. Loss of intimate contact—for example through gap formation (particularly if moist) or the presence of intervening materials—raises the likelihood of crevice-type corrosion. Corrosion has often been observed where foreign materials (e.g., wood) were left at the interface and exaggerated the process due to the lower PH-value compared to concrete. Corrosion may also be initiated by construction deviations such as cavities at the liner interface, or by carbonation and/or chlorides reaching the liner.

Corrosion risk is elevated at material transitions and geometric discontinuities, where water and organic debris can accumulate. Defects that disrupt passivity—such as voids—increase risk; such voids may originate from casting deficiencies or may develop secondarily as corrosion progresses.

When steel corrodes, rust is formed. In moist concrete, part of the corrosion products may dissolve and be transported through the concrete pore structure and cracks, as well as through any existing gaps. If the corrosion products are not removed by transport, they can exert significant expansive pressure on both the steel and the surrounding concrete. Cracking of the concrete cover over reinforcing bars is evidence of the high pressures that can develop. Surface staining of concrete and the formation of gaps between concrete and reinforcement in submerged structures indicate that a portion of the corrosion products can dissolve and be transported. Locally, the resulting pressure may cause cracking in the concrete and buckling of the liner plate. The corrosion products can expand to roughly 2–6 times the original steel volume, generating internal pressure that can lead to cracking or spalling of adjacent concrete and facilitate further transport and redistribution of corrosion products (Sandberg, 2019).

A key consequence of gap formation is that it can create an environment where corrosion can start and then propagate. This may locally reduce the liner thickness and, in severe cases, lead to through-wall penetration.

For corrosion to initiate, three conditions must be fulfilled:

1. A driving force (potential difference) between anodic and cathodic areas on the steel surface.
2. An electrolyte, i.e., a conductive liquid film—typically moisture containing dissolved ions (e.g., salts/chlorides).
3. An electron acceptor, normally oxygen, to sustain the cathodic reaction.

A cavity at the steel–concrete interface can satisfy these conditions. If the cavity is sealed, it must be sufficiently large—and/or receive enough oxygen by diffusion through the concrete—for corrosion to be sustained at a significant rate. Corrosion propagation is more likely if the cavity has direct access to air, for example through a liner–concrete gap, a major crack, or an embedded penetration/pipe. In addition, the cavity typically needs to be partially water-filled to provide an electrolyte; if oxygen availability is low, both the probability of initiation and the corrosion rate generally decrease.

For BWR containments, the initiation risk is generally lower because the containment atmosphere is nitrogen-filled during operation, reducing the availability of reactive gases at the inner wall and leading to more favorable passivation conditions and slower corrosion propagation than in PWRs, where the containment is not nitrogen-filled. Furthermore, the outer wall exposure conditions differ: BWR outer walls are typically influenced by indoor building climate, whereas PWR outer walls are more directly exposed to outdoor climate. These factors contribute to a theoretically lower liner corrosion risk in BWRs. In an Energiforsk-related assessment, several critical areas were identified; Figure 21 highlights corrosion-prone locations for BWR and PWR containments (Sandberg, 2019).

If a gap exists between steel liner and concrete, three cases can be distinguished with respect to corrosion impact:

1. Closed cavity: Water and oxygen may be transported through the concrete. There is a risk of waterline corrosion.
2. Externally connected cavity: The gap communicates with the external environment; conditions resemble a cavity connected through an air-filled channel.
3. Leakage-water pathway: The gap enables transport of pool leakage water along and past the interface. Here, passivity conditions deteriorate because deionized water leaches hydroxide ions. Passivity can be lost even without CO_2 access, while oxygen can be supplied via dissolved oxygen in the water; the corrosion rate is governed by the oxygen content.

a)

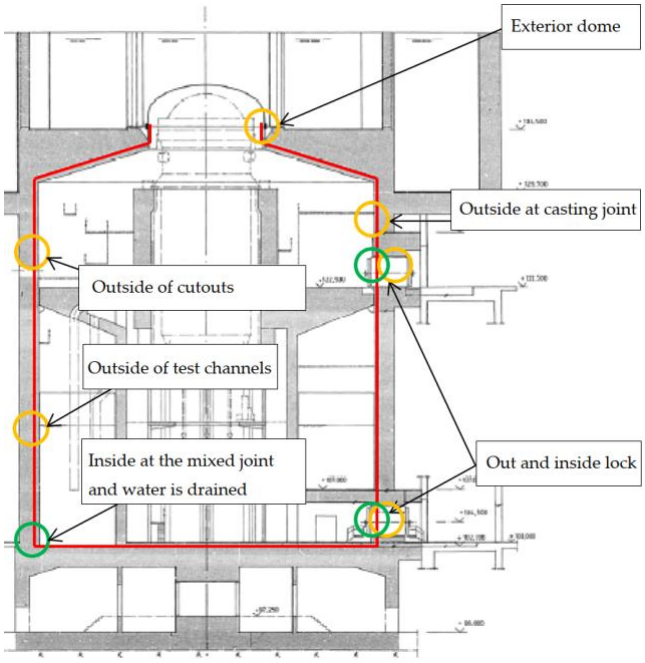

b)

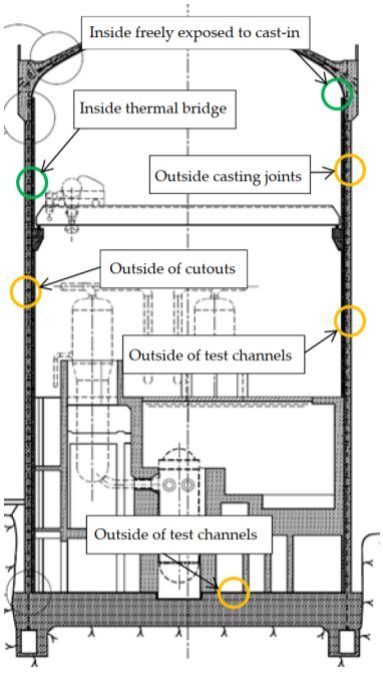

Figure 21. (a) Points at risk for corrosion on the steel liner in a BWR. (b) Points at risk for corrosion on the steel liner in a PWR (Sandberg, 2019).

3.2 CARBONATION AND CHLORIDE INGRESS

Corrosion of a steel liner cast into nominally "defect-free" concrete can occur due to carbonation of the concrete and/or chloride ingress. Carbonation is a process in which atmospheric carbon dioxide reacts with calcium hydroxide in the concrete to form calcium carbonate. This reaction reduces the pH of the carbonated concrete, which can depassivate embedded steel and initiate corrosion (Malm et al., 2021). However, carbonation is generally slow, and given the large wall thicknesses in containment structures, the carbonation front is not expected to reach the steel liner within a reactor's service life if the concrete is free from defects. Additionally, BWR containment vessels are filled with nitrogen during operation, meaning the inner wall is exposed to CO_2 mainly during service periods (approximately one month per year), and process water is deionized, which further limits chloride exposure (Sandberg, 2019).

Chloride ingress in nuclear containment concrete is also typically slow due to the concrete's dense, low-permeability microstructure. The main corrosion risk related to carbonation and chloride ingress arises when cracks, voids, or penetrations provide pathways for air and/or water transport through the concrete to the steel liner. Under such conditions, corrosion may initiate and progress over time, potentially contributing to gap formation between the steel liner and the surrounding concrete due to the volumetric expansion of corrosion products.

3.3 MOISTURE TRANSPORT

Moisture transport in concrete is a complex process governed by factors such as relative humidity, temperature, and material properties. When moisture transport through a concrete wall is significant, condensation may occur in cavities within the concrete or at the interface between the concrete and a steel liner. If a cavity exists on the inner side of the steel liner and a thermal bridge forms through the outer wall, substantial condensation can develop (Sandberg, 2019).

Condensation in a larger, partially air-filled cavity caused by moisture transport through the concrete increases the risk of steel liner corrosion and may contribute to gap formation through the expansion of corrosion products, as discussed in Chapter. 3.1.

For nuclear reactor containment structures with steel liners, moisture transport is critical because it can affect structural integrity, primarily by altering material properties which govern creep and shrinkage of the concrete. Drying of loaded concrete increases the combined effect of drying shrinkage and creep. Furthermore, increased moisture transport through the containment wall (or local regions of it) may lead to non-uniform creep or shrinkage across the wall thickness and between wall sections, which could contribute to the development of gaps between the steel liner and the concrete. The implications for gap formation are discussed further in the following sections.

3.4 SHRINKAGE, CREEP, AND TEMPERATURE EFFECTS

Concrete shrinkage begins after casting. In nuclear containment structures, drying and shrinkage progress extremely slowly. Studies of Swedish reactor containments (see Chapter. 2.2) show that the containment wall is still drying after many years. Climatic measurements in BWR and PWR containments indicate that, even after 30–50 years of operation, shrinkage continues. This slow drying is attributed to the large wall thickness and one-sided drying due to the steel liner (Lundqvist, 2012) .

Concrete shrinkage is considered a function of moisture loss and is related to a reduction in moisture content in the concrete pore system. Shrinkage therefore primarily results from contraction of the cement paste as water leaves the pores; this component is traditionally referred to as drying shrinkage. Shrinkage also occurs due to cement hydration, referred to as autogenous shrinkage.

Shrinkage is not uniform through the containment wall because the wall surfaces are exposed to different climatic conditions. This creates a shrinkage gradient through the wall, causing uneven internal stresses in the cylindrical wall, with tensile stresses near the drying surface. The non-uniform shrinkage can be inferred from the relative-humidity variation through the wall, see Figure 9, and is likely to cause larger shrinkage strains toward the inner surface compared with the surface adjacent to the steel liner.

A hypothesis is presented in Chapter. 2.3.2 that the observed gaps in Swedish reactors may originate from shrinkage effects. The mechanism can be illustrated using a beam analogy with fixed supports, see Figure 22a. If the beam is subjected only to a moisture gradient (wet at the lower surface and dry at the upper surface), the resulting shrinkage gradient induces curvature, bending the beam downward. Applied to the containment wall, this corresponds to opening along the boundary due to beam-like behavior. If the beam is then cut at midspan, the outer boundary of the opening behaves as two cantilever beams with tensile stresses on their upper surfaces; these stresses bend the cantilevers upward, see Figure 22b. A similar condition can be expected in the inner cylindrical wall: surface stresses around an opening may bend the cylinder wall away from the liner.

In contrast, the outer concrete cylinder is expected to press against the steel liner around the opening due to creep and shrinkage strains, so no gap would form between the outer concrete cylinder and the liner. This is consistent with observations in Swedish reactors, Chapter. 2.3, where through-wall openings have been made. To further support this hypothesis, measurements capturing the containment-wall response before, during, and after forming an opening should be performed and evaluated.

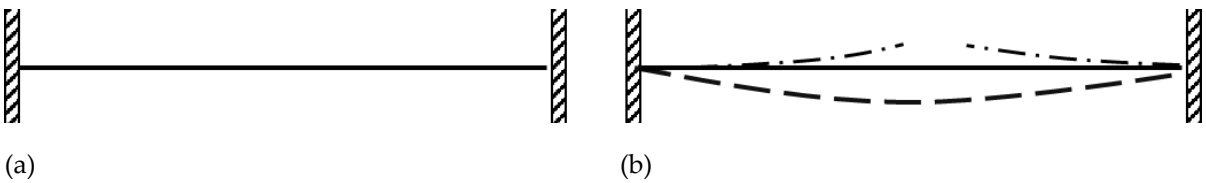

Figure 22. (a) Shrinkage deformation effects on a restrained concrete beam, illustrating the effect of a steel liner in a concrete cylinder wall. (b) Shrinkage-induced deformation of a partially restrained concrete beam, illustrating the effect of a cut steel liner in a concrete cylindrical wall.

3.5 GEOMETRIC EFFECTS AND CUT-OUTS

The severity of a gap between a steel liner and the surrounding concrete depends mainly on the gap width, the delaminated area, and the gap's location. Geometrical effects and cut-outs of the steel liner have the potential to affect the risk of gap formation.

As summarized in Chapter 2.3, gaps have been observed in Swedish reactors following openings made through the containment wall. At Ringhals 2–4, inspections documented gaps of approximately 1–5 mm between the steel liner and the inner containment wall adjacent to the openings. Notably, all reactors with reported gap formation are of type PWR. It remains unclear whether these gaps formed as a result of the wall-opening, or whether they pre-existed. If the gaps existed prior to the wall opening, an assessment is needed to determine whether a gap on the order of 1–3 mm is significant. Reference criteria from the literature are therefore sought to indicate when a liner–concrete gap becomes a concern, both with respect to corrosion risk and containment structural integrity. To date, no such generally applicable reference value has been identified.

The hypothesis in Chapter 2.3.2 - that gap observations made after cutting openings may be influenced by the opening procedure - is also considered. Openings are typically made by drilling a line of large concrete cores, see Figure 13. In some cases, coring is performed through the full wall thickness including the liner; in others, coring is performed from both sides, see Figure 16, and the liner is cut separately. Coring can affect liner–concrete interaction near the opening through drilling thrust (contact pressure) and vibration.

For the Ringhals 2 opening during dismantling, coring from the outside was used. If the inner concrete wall was removed first, leaving the liner free on the inside, then after penetrating the outer wall and liner the drill would have imposed inward pressure and vibration on the liner, potentially affecting local bond and liner deformation. The drilling forces are unlikely to deform the inner concrete cylinder around the opening (≈300 mm width) due to the wall's high stiffness. However, if uneven shrinkage, see Chapter. 3.4, had already caused inward bending of the inner cylindrical wall, drilling could have contributed to increased gap formation around the opening. Assessing this requires measurements from containment wall-opening operations.

Holes such as for casing pipes and manholes introduce local liner cutouts. The principle, see Figure 23, is that the pipe is welded pressure-tight to the liner, typically also fitted with shear connectors. In practice, cutouts are often formed using blockouts during slipform casting; after casting and liner positioning, the liner openings are cut, pipes with flanges are welded to seal them, shear connectors are installed at the penetration, and the blockouts are reinforced and casted. These attachment points are usually designed to be stronger than the pipes themselves (Roth et al., 2002). While penetration design is outside the scope of this study, the risk of gap formation around liner openings is discussed.

Where no shear connectors are used, composite interaction between steel and concrete relies on chemical adhesion and friction to transfer shear at the interface. Once slip occurs, chemical adhesion is degraded (Bradford et al., 1995).

It is therefore important to know the interface shear stress level at which adhesion is lost. Experimental findings have shown that the adhesive strength between steel sheets and concrete for an untreated surface is at least 0.75 MPa; these experiments were conducted on non-corroded steel plates (Berthet et.al., 2011).

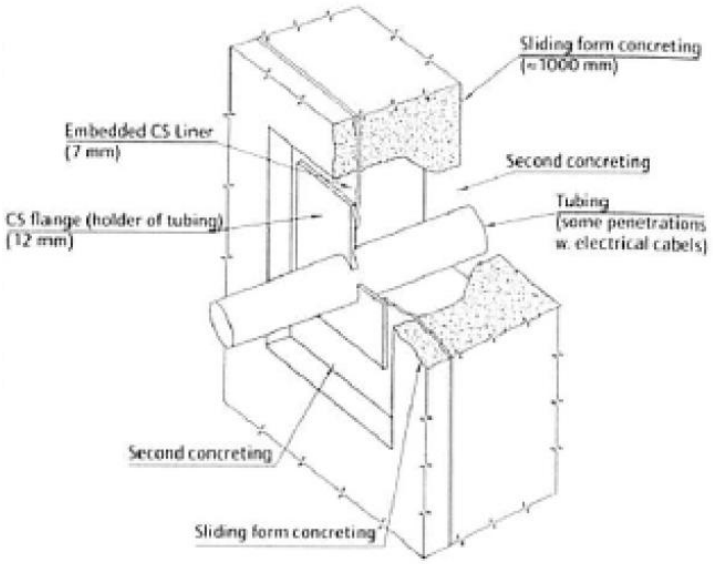

Figure 23. Principal concept of steel liner cutouts for casing pipes and manholes (Sandberg et.al., 2019).

4 Methods: Gap formation simulations – Case study

The purpose of this case study is to simulate the short- and long-term material effects that might poses risk of gap formation between the steel liner and the concrete walls of reactor containment buildings. A generic Nordic PWR reactor, resembling Ringhals II geometry, has been selected for the analysis because its containment structure is exposed to outdoor conditions.

The study centers on literature review, analytical calculations, and numerical simulations to identify critical factors contributing to gap formation and its effects. Comparison on measured data and literature is made for the analytical and FE-calculation to evaluate consequences and try to conclude the causes of gap formation between steel liner and cylinder wall and its effects.

4.1 CASE STUDY ASSUMPTIONS

Several assumptions are made to simplify and conduct the analytical and numerical calculations:

- Only the cylindrical containment wall is considered. Exclusion of the floor slab and roof cupola is made in calculation and FE modelling due to limiting time within the project.
- Only horizontal tendons are considered due to time constraints and that the effect of vertical tendons is proven to be small, as presented in Chapter. 2.4.2.
- Linear elastic material models have been made.
- Analytical calculations are based on Eurocode 2 models.
- Limitations in terms of material models have been made. Despite that all information has not been available, all assumptions regarding material properties and climate conditions have been made as average values and should, therefore, be representative for the typical containment building in Sweden and Finland.
- Outer and inner containment walls are treated as separate in calculations as discussed in Chapter. 1.4.

4.2 CASE STUDY DEFINITION AND GEOMETRY

By reviewing Swedish and Finish reactor containment buildings for both BWR and PWR, geometry and climate conditions have been chosen to analysis and further study short- and long-term effects.

To evaluate the effect of concrete hardening and behavior and response, several different scenarios are checked for reactor type PWR. Different zones within the reactor are studied due to temperature and climate variations for both inner and

outer containment wall. This is done by evaluating short- and long-term effects for containment walls and critical sections for the steel linear.

All containments in Nordic nuclear power plants are constructed somewhat uniformly, featuring a load-bearing outer shell made of reinforced and post-tensioned concrete as discussed in Chapter. 2.1. Inside this load-bearing outer layer, there is a steel liner, followed by an inner missile protection layer composed of reinforced concrete. However, the construction stages and geometry of the containment buildings differs. Due to this a case study for a general reactor containment building is made, furthering a critical scenario for the formation of a gap between the steel liner and concrete. To determine a representative containment structure geometry, all Nordic PWR containment buildings have been studied and a geometry that is representative as what is thought to be a critical scenario for gap formation to form has been chosen.

4.2.1 Geometry

The geometry of Swedish and Finish containment structures is presented in Chapter. 2.1. The chosen geometry for the cylindrical containment wall of the case study is summarized in Table 3 and illustrated in Figure 24. The parameters chosen are based on a general scenario to investigate the causes and effects of gap formation between the steel liner and concrete, closely resembling the geometry of PWR at Ringhals II.

Table 3. Geometry of cylindrical containment wall used in the case study.

Part of containment building	Thickness [mm]	Height [m]	Internal diameter [m]
Inner containment wall	300	59	35,4
Steel liner	7	59	36
Outer containment wall	800	59	36,014

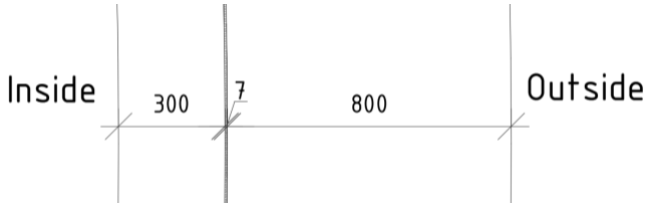

Figure 24. Section of cylindrical containment wall used in the case study; measurements given in mm.

4.2.2 Analysis sequence

The sequence in which effects and loads are applied is important for the analysis of gap formation effects. As studied in Chapter. 2.1.1 the containment construction involves counter-casting steel and concrete as well as grouting between concrete and steel. The case study aims to examine for which geometries and construction methods there is a risk of gap formation, if there is one. Therefore, an analysis sequence based on Chapter. 2.1.1 is chosen which is deemed to have a negative impact on the possibility of gap formation, which occurs when the concrete for the outer and inner containment wall has been cast against the steel liner. This is because post-injection provides a direct counteraction when the initial effects of casting for the inner and outer wall have subsided.

Following analysis sequence is to be studied, assumption of simultaneous casting of inner and outer wall is made:

0. Initial conditions at time t = 28 days at time of cured concrete inner containment wall.
1. Conditions at time t = 28 days at time of cured concrete outer containment wall.
2. All tendons are prestressed at time t = 365 days. Strain in tendons and resulting ε_s due to pree-stress is applied to tendons and resulting reduction of concrete radial diameter.
3. Material effects after tendons are tensioned, creep and shrinkage at time t = 1 year and 50 years and relaxation of tendons.
4. Temperature field and varying climate conditions is applied for different scenarios presented in Chapter. 2.2.

4.2.3 Climate conditions

To determine the initial conditions and the long-term effects on concrete the construction stages have been analyzed in Chapter 2.1.1.

To calculate creep and shrinkage at various times after construction, the RH profile through the wall thickness is required so that shrinkage can be evaluated for each section. To avoid detailed moisture modelling, the Eurocode 2 shrinkage calculation is used based on RH measurements reported by Oxfall which estimates the development of RH profiles within containment walls.

Table 4, presents the average RH in the concrete walls of a PWR over different time periods, based on the moisture profiles presented by Oxfall, see Chapter. 2.2. Table 4 also lists the corresponding final shrinkage strain at equilibrium calculated using the Eurocode 2 shrinkage model for each RH level.

Table 4. Climate conditions for a PWR - estimated average RH within the containment walls and the corresponding final shrinkage. Values are approximations based on the research by Oxfall (Oxfall, 2016).

	RH - Inner containment wall [%]	Final shrinkage – Inner containment wall [‰]	RH - Outer containment wall [%]	Final shrinkage - Outer containment wall [‰]
t = 28 days	90	0,149	90	0,149
t = 365 days	80	0,208	85	0,180
t = 50 years	70	0,254	80	0,208

4.2.4 Material properties

Material properties of concrete are retrieved from Energiforsk report on compilation of concrete test data from the nuclear industry (Roth, T., Silfwerbrand, J., Sundquist, H., 2002), and the summary of construction and materials of Swedish nuclear power plants (Zaraei & Lundqvist, 2021). The concrete used in the casting of most Swedish and Finish nuclear reactors was specified to correspond to

strength class K40-K50. The material properties in Table 5 are therefore selected as representative values.

Table 5. Material properties of concrete used in case study.

	Inner/outer containment wall:
Concrete Class	Class I, K50 (C40/50)
Cement	Std
Max. Aggregate Size	32 mm
Additives	Yes
Water-Cement Ratio (w/c)	0.42
Aggregate	Gravel, sand, and stone
Aggregate Rock Type	Gneiss
Mean compressive strength - f_{ck}	40 MPa
Mean elastic modulus - E_{cm}	35 GPa

Material properties used in the case study for the tendons are given in Table 6 and are based on a compilation of concrete test data from the nuclear industry (Roth et al., 2002). Vertical tendons are excluded due to time constraints and because vertical prestressing has a negligible effect on the radial deformation and strains investigated in this study.

Table 6. Material properties of tendons used in the case study.

	Horizontal tendons
Post-tensioning force [MN]	4.8
Post-tensioning stress - σ_p [MPa]	1200
Number of horizontal tendons per meter of wall height	3

4.2.5 Boundary conditions and studied sections

To evaluate the case study, the containment cylindrical wall is modelled over its full height, without the roof and floor structures, and a wall segment at mid-height is selected for assessment. This is done to minimize the influence of boundary-condition effects on the results. The upper and lower boundaries are restrained from movement in the x-, y-, and z-directions. The studied sections and applied boundary conditions for the uncracked concrete load case are shown in Figure 25.

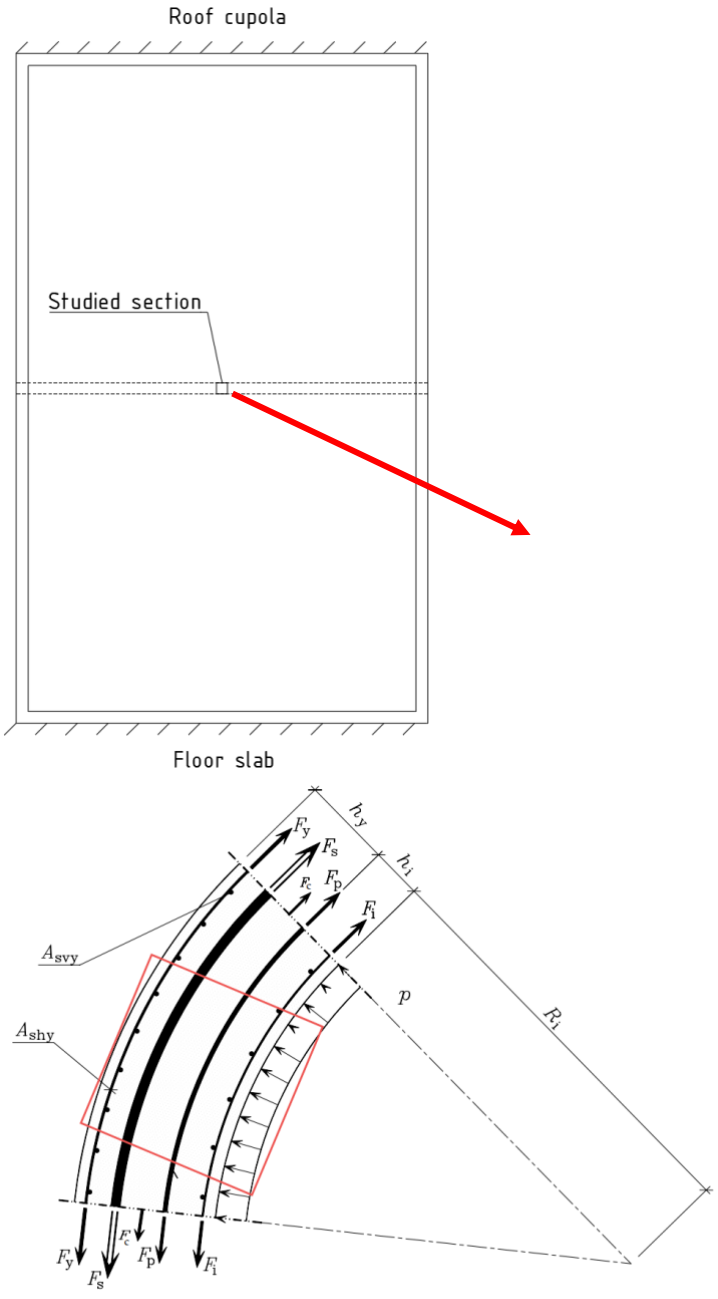

Figure 25. Containment wall boundary condition and studied section, reproduced with modifications from (Roth et.al., 2002). The red markings indicate the studied section, 1 m in width and 1 m in height.

4.3 ANALYTICAL MODELS AND ASSUMPTIONS

To determine short- and long-term effects for different scenarios within the containment building, calculations are performed for the selected case-study geometry presented in Chapter. 4.2. Creep strains, shrinkage strains and effective modulus of elasticity for the concrete are computed using the Eurocode 2 method (CEN, 2014). The modelling approach is summarized as follows.

In the case study, the Eurocode 2 method is used with the measured data presented by Oxfall in Chapter. 2.2.4. Since the measurements represent an average through the wall section, the Eurocode 2 time-development factor is not applied; instead, the concrete section is assumed to have reached the final shrinkage value corresponding to the average RH in the wall section.

The method can be summarized as follows:

- **Shrinkage calculations using average RH from measurements (equilibrium response).**
  Measured average RH over time in the containment wall is used as input, and the final (equilibrium) shrinkage strain is calculated using Eurocode 2.

The reason this method is used instead of the Eurocode 2 time-development function for shrinkage is that the Eurocode 2 approach is a general, empirical model, whereas Oxfall's measurements provide a site-specific description of shrinkage development over time through the recorded relative humidity in the walls. This is well suited to the case study, since it considers a generic reactor building assumed to be located in Varberg, where local environmental conditions are better represented by the measured RH data than by a purely generic time-development formulation.

Creep is determined using the time-dependent creep coefficient, φ. In the Eurocode 2 model, φ depends on the concrete age at loading, t_0; the concrete compressive strength (via a modified modulus of elasticity); and the ambient relative humidity. A detailed description of the calculations is provided in Appendix A: Hand calculations – Creep and shrinkage.

4.3.1 Assumptions

- All time-dependent properties such as creep and shrinkage in the concrete and relaxation in tendons are calculated at the age of 28 days, 1 year and 50 years.
- Prestressing of tendons is assumed to take place 1 year after casting with all tendons tensioned simultaneously.
- Creep and shrinkage strains are calculated using the Eurocode 2 functions with the measured average RH in the containment walls, see Table 4, assuming that the concrete section has reached the final shrinkage corresponding to the RH level in the wall. This provides a simplified representation of the wall's drying behavior over time.

4.3.2 Shrinkage

The total shrinkage strain is composed of two components: the drying shrinkage strain and the autogenous shrinkage strain that is calculated according to SS-EN 1992-1-1 - 3.1.4 (CEN, 2014). The drying shrinkage strain develops slowly since it is a function of the migration of the water through the hardened concrete.

part therefore develops in the early days after casting. Autogenous shrinkage is a linear function of the concrete strength and is calculated using Eq. (3).

$$\boldsymbol{\varepsilon_{cs} = \varepsilon_{cd} + \varepsilon_{ca}} \qquad (1)$$

ε_{cs} is the total shrinkage strain

ε_{cd} is the drying shrinkage strain

ε_{ca} is the autogenous shrinkage strain

Drying shrinkage:

The development of the drying shrinkage strain in time related to the relative humidity follows from SS-EN 1992-1-1 3.1.4 and Appendix B2 in Eq. (2) (CEN, 2014). For the inner containment wall, concrete surface on the inside is coated with a moisture-tight epoxy barrier, making the drying shrinkage process very slow. In calculations the epoxy barrier is included for the inside of the inner containment wall by using the average RH in the wall sections at different times, thus considering the very slow drying process through the epoxy membrane. See Appendix A for calculation of drying shrinkage.

$$\boldsymbol{\varepsilon_{cd}(t) = \beta_{ds}(t, t_s)\, k_h\, \varepsilon_{cd,0}} \qquad (2)$$

Autogenous shrinkage:

Autogenous shrinkage occurs due to water consumption in the chemical curing process and is time dependent. The autogenous shrinkage is approximated from SS-EN-1992-1-1 3.1.4, Eq. (3) (CEN, 2014). See Appendix A for calculation of autogenous shrinkage.

$$\boldsymbol{\varepsilon_{ca}(t) = \beta_{as}(t)\, \varepsilon_{ca}(\infty)} \qquad (3)$$

4.3.3 Creep

Creep of concrete is defined using the model in Eurocode 2. In this model, the creep is described by a creep coefficient, $\varphi_c(t, t_0)$ and is calculated according to Eq. (4).

$$\varphi_c(t, t_0) = \varphi_0 * \beta_c(t, t_0) \qquad (4)$$

where φ_0 is the nominal creep value and $\beta_c(t, t_0)$ is a coefficient that describes the development of creep over time after loading. For a complete description of the creep, refer to Eurocode 2 (CEN, 2014).

The creep strain, ε_{cr}, is included using equation (5). Where σ_c is the compressive stress in the concrete.

$$\varepsilon_{cc}(\mathrm{t}, t_0) = \rho_c(t, t_0) * \frac{\sigma_c}{E_{eff}} \qquad (5)$$

Creep is only considered in areas where prestress is present (i.e. the outer cylinder wall) where stress from the prestress is dominant. Accordingly, σ_c in Eq. (5) is matched with the concrete stress equivalent to the prestress in horizontal orientation, while all additional components remain at zero. Concrete is compressed vertically and horizontally with a creep strain corresponding to the

tension force from tendons acting on the section, the strain is calculated using the effective creep coefficient. In the case study the vertical tendons have been excluded in calculation.

4.3.4 Temperature

Thermal strains ε_{tr} are assumed linearly dependent on the temperature state following Eq. (6) where α is the constant linear coefficient of thermal expansion set to be $\alpha = 10^{-5}K^{-1}$, and T_{ref} is a reference temperature at which the material is stress/strain free set to between 5-25 °C which corresponds to assumed outdoor temperature surrounding the containment wall at casting. Temperature T is taken from the spatial field summarized in the thermal analysis described in Chap 2.2.

$$\varepsilon_{th} = \alpha_c(T - T_{ref}) \qquad (6)$$

4.3.5 Steel tendons

Deformation from cable tensioning is calculated at initial stage without relaxation from cables and at time t = 50 years with relaxation of cables. The constitutive behavior of the steel tendons is given in Eq. (7) for the total strain ε, in steel tendons at a given time. The total strain ε, is the initial instantaneous strain ε_{pi} due to the prescribed prestress force, minus losses due to relaxation of tendons, ε_{pr}. The thermal strains and frictional loss of tendons are set to 0 as a simplification. The relaxation strain ε_{pr} is approximated from EC2 (CEN, 2014) to a relaxation loss of 2.5% after 50 years. The instantaneous strain depends on where in the containment the tendon is located but is here assumed to have a uniformly tendon force over a cross-section height of 1 meter for the middle height of the reactor.

$$\varepsilon = \varepsilon_{pi} - \varepsilon_{pr} \quad (7)$$

4.4 ANALYTICAL CALCULATIONS

Detailed calculations are presented in Appendix A. The procedure of the calculations, times from Chap. 4.2.2 and results are presented for different scenarios.

At time t = 28 days drying effects for the inner and outer containment wall are considered. At time t = 1 year tendons are assumed to be tensioned and resulting strain is analyzed. At that time, the initial effects of concrete will have decreased the radius of the inner and outer containment wall due to shrinkage effects. When tensioning the tendons in the outer containment wall, the radial diameter of the concrete wall will decrease, resulting in a reduction of any gap between the steel liner and outer containment wall that might have formed. Over time, the cable tension decreases due to the relaxation of tension cables, which results in the radial diameter increasing, however, shrinkage continues with a radial decrease in radial diameter over time.

4.4.1 Total deformation

The elastic strain, ε_{el} , corresponds to the difference between the total strain, ε_{tot} , and the inelastic strains that is non-reversible, ε_{inel} and is described by Hooks law according to Equation. (8).

$$\varepsilon_{el} = \varepsilon_{tot} - \varepsilon_{inel} = \frac{\sigma}{E} \quad (8)$$

The total strain, ε_{tot}, is described by Equation. (9) and is calculated initially and for long term loading by tension force from tendons, it is the sum of the elastic strain, ε_{el}, the thermal strain, ε_{th}, shrinkage strain, ε_{sh} and creep strain, ε_{cr}.

$$\varepsilon_{tot} = \varepsilon_{el} + \varepsilon_{th} + \varepsilon_{sh} + \varepsilon_{cr} \quad (9)$$

The total strain is calculated using a modified modulus of elasticity described in Equation. (10), which considers the effect of creep in concrete. The effective creep value is calculated for a given time and reduces the stiffness of the concrete.

$$E_{c.eff} = \frac{E_c}{(1+\varphi_{eff})} \quad (10)$$

Creep and shrinkage tangential strains are calculated for a horizontal section as shown in Figure 25 with the horizontal tendon force. To evaluate the radial displacement Equation. 11 is used, where the total radial displacement, Δ_r is calculated from the radius of the concrete cylinder wall, r and the total strain, ε_{tot}.

$$\Delta_r = \boldsymbol{\varepsilon_{tot}} * \mathbf{r} \quad (11)$$

4.4.2 Analytical calculations - outer containment wall

Total strain in the outer containment wall is evaluated over a 50-year period by combining shrinkage, creep, and temperature effects, to compare the early-age state (28 days) with long-term behavior (1 year and 50 years). Long-term creep is represented by using a reduced (time-dependent) effective modulus of elasticity for the concrete. The analysis is performed for a section with horizontal tendons; vertical creep from self-weight is therefore neglected as it is assumed to have minor influence.

Figure 26 presents the horizontal tangential strain. At 28 days, the initial strain is primarily due to autogenous shrinkage and the early stages of drying shrinkage. At prestressing (365 days), the tendons reduce the wall radius, compress the concrete cylinder and close any shrinkage-induced gap that may have formed between the concrete and the steel liner. At 50 years (18250 days), creep increases as the concrete stiffness decreases with time, although tendon relaxation also occurs.

The absolute (total) horizontal tangential strain is shown in Figure 27. The total strain is negative because tendon-induced creep and shrinkage both reduce the radius of the outer concrete cylinder. Relative humidity in the wall decreases over time, albeit slowly. Temperature variations add further strain: higher temperatures increase tangential strain, and lower temperatures decrease it (e.g., during winter or outages). Temperature also varies with elevation, as the heat source is typically located higher in the reactor.

Using a reference temperature of 10°C, the mid-height tangential thermal strain is estimated to increase by up to 200 μ-strain at 30°C and decrease by about 100 μ-strain at 0°C.

The results indicate that, for defect-free concrete, no gap is expected to form at the contact zone between the steel liner and the outer containment wall due to short- or long-term effects. After 50 years, the total tangential strain decreases by about 470 μ-strain, corresponding to a tangential shortening of 0.47 mm over 1 m. Using Equation 11 and the average outer wall radius, this gives a radial displacement of approximately 9 mm.

If cable detensioning is performed, elastic deformation is recovered upon unloading, while creep recovery is slow and difficult to quantify. Even with detensioning, the concrete cylinder will have shrunk over time; after 50 years the tangential displacement is calculated as 0.21 mm over 1 m (208 μ-strain), corresponding to a radial displacement of about 3.8 mm (Equation 11). Thus, even after tendon relaxation, the outer concrete wall is expected to remain in contact with the steel liner, preventing gap formation in defect-free concrete.

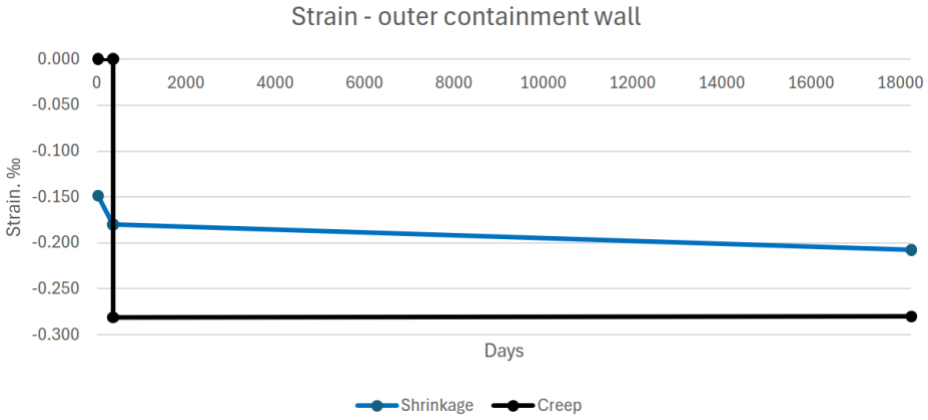

Figure 26. Tangential strain from shrinkage and creep for outer containment wall over 50 years.

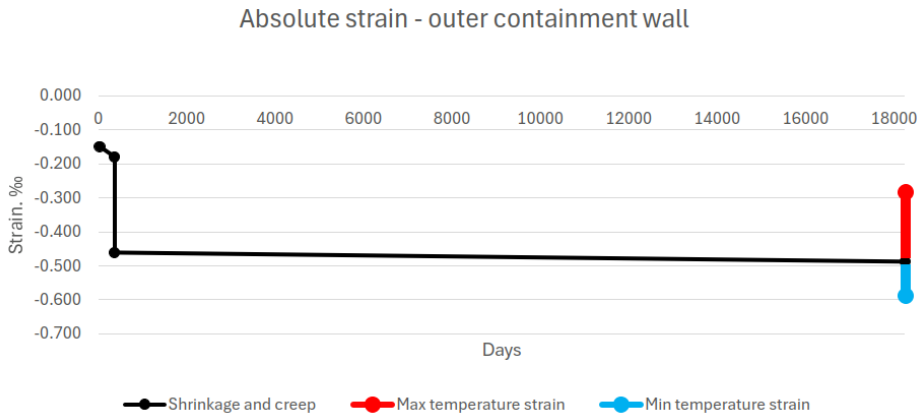

Figure 27. Absolute tangential strain from shrinkage and creep for outer containment wall over 50 years. Red line represents the maximum temperature strain and blue line is the minimum temperature strain affecting the containment wall.

4.4.3 Analytical calculations - inner containment wall

Total strain in the inner containment wall is calculated over 50 years from shrinkage, creep and temperature, using the same framework as for the outer wall but with different boundary conditions. The inner face is assumed to be covered by a low-permeability membrane (paint/epoxy), which acts as a moisture barrier. After casting/grouting against the steel liner, the wall is treated as effectively sealed toward the liner and membrane-controlled toward the reactor interior. These assumptions imply very slow internal drying and are used to define the humidity boundary condition for drying shrinkage.

The strain history is presented in Figure 28. The tangential strain at 28 days is primarily due to autogenous shrinkage and the early stages of drying shrinkage. Vertical creep at the initial state is not included, since it would be driven primarily by self-weight of the wall/roof and is considered outside the scope of the tangential section assessment. Because the inner wall is not prestressed, the tangential strain development is governed by shrinkage-induced radius reduction, with the rate controlled by the low-permeability inner surface condition. As shown in Oxfall's study (Oxfall M., 2016), the initial drying shrinkage effects have the largest impact on strain over 50 years. The relative humidity remains high over a long time when the temperature is controlled.

For long-term shrinkage over 50 years, wall drying is approximated using the data presented in Chapter. 2.2.4, where drying conditions in the wall are used to estimate the development of shrinkage strain. Appendix 1 provides the corresponding shrinkage calculations at 28 days, 1 year, and 50 years, and the resulting tangential strain is plotted in Figure 28. Temperature effects are shown as brackets (“staples”) to illustrate how a long-term reactor shutdown temperature change would add thermal strain. The radial displacement at reference temperature after 50 years is then by Equation. 11 ca 4,5mm with the average radius of the inner containment wall used.

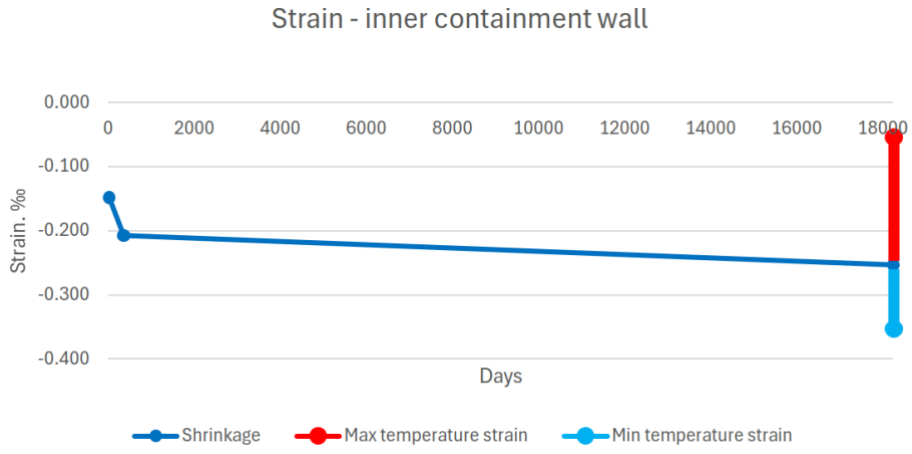

Figure 28. Strain from shrinkage and creep for inner containment wall over 50 years. Red line represents the maximum temperature strain and blue line is the minimum temperature strain affecting the containment wall.

To quantify the effect of reinforcement on shrinkage in the inner containment wall, reinforcement restraint is included in the shrinkage strain calculation. Reinforcement is treated as providing stiffness-based restraint that reduces the

concrete's free shrinkage strain, acknowledging that the result is time-dependent and influenced by creep, bond conditions, and potential cracking; therefore, the approach is used as an approximation.

The approximation is based on the following assumptions:

- Perfect bond between concrete and steel (no slip).
- No cracking.
- Free concrete shrinkage strain, ε_{sh}, is shared between concrete and reinforcement according to their axial stiffnesses EA.

Under these assumptions, where $E_c * A_c$ are the concrete modulus and area of the section, and $E_s * A_s$ are the reinforcement modulus and total steel area in the section, the effective (constrained) shrinkage strain for the composite section is estimated by Equation (12):

$$\varepsilon_{sh.eff} = \varepsilon_{sh} * \left(\frac{E_c * A_c}{(E_c * A_c + E_s * A_s)}\right) \quad (12)$$

For the inner wall reinforcement layout s200 ϕ32 on both faces, the calculation gives an effective shrinkage strain of approximately 84% of the free (unrestrained) shrinkage strain over 50 years. Given a total strain after 50 years to be ≈ 0,25 μm/m, indicating that the reinforcement ability to constrain shrinkage placed in the inner containment wall have a small reduction of total strain.

4.5 FINITE ELEMENT MODELLING

To further assess long-term behavior and the potential for gap formation between the steel liner and the concrete, a finite element (FE) model is established in ABAQUS (Brigade/Plus). The model represents the containment as two concentric concrete cylinders (inner and outer wall) over the full reactor building height, providing a simplified but representative structural idealization. The FE results in terms of strain development and deformations are evaluated over time and compared with the corresponding hand calculations to verify consistency.

4.5.1 Model setup

The same conditions as used for the hand calculations are applied in the FE analyses; geometry and material properties are given in Chapter. 4.2. The cylindrical concrete walls are modelled using solid elements, while the steel liner is represented by shell elements, with properties according to Table 3. The model is configured to simulate 50 years of shrinkage and creep for both the inner and outer concrete cylinders. Only creep associated with prestressing is included.

The FE model is developed under the assumption of axial symmetry and is intended to represent the behavior of a typical vertical section of the containment. With this simplification, several features of the real structure are not captured, such as the stiffening effect of the spent fuel pool and buttresses, as well as local influences from personnel and equipment penetrations.

The cross-section shown in Figure 29 (a) is revolved to create a three-dimensional model, where the lower and upper boundaries are restrained in the global x-, y- and z-directions. Shrinkage and creep loads are introduced via equivalent temperature loads applied to the inner and outer surfaces (indicated in red in Figure 29 (b). Figure 30 shows the mesh used in the analysis, including the evaluated ring segment with a height of 1 m. The element size is 0.30 m in the outer wall and 0.15 m in the inner wall.

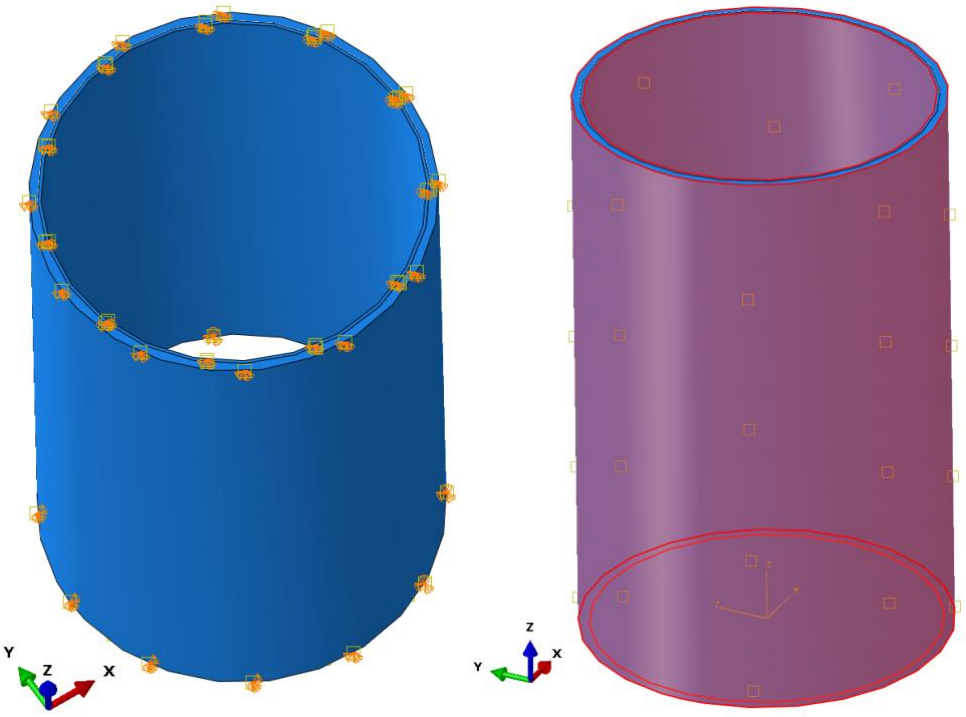

a) b)

Figure 29. Illustration of modelled containment wall with outer and inner concrete cylinder and steel liner between. Boundary conditions shown in (a) and surface of load application shown in (b).

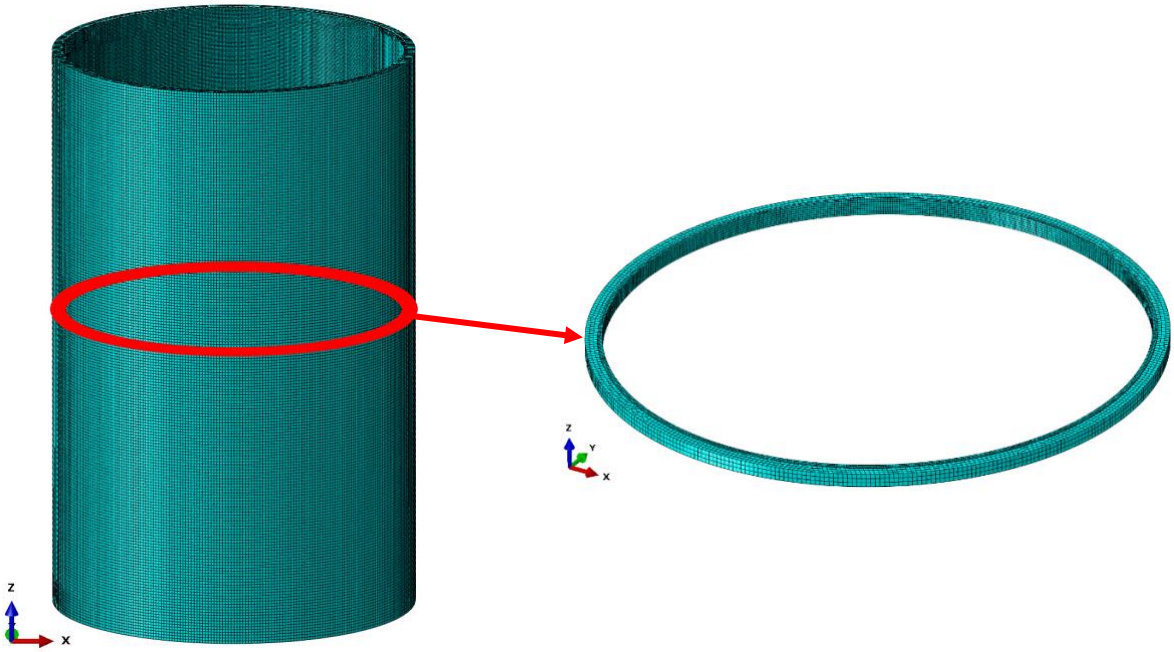

Figure 30. Illustration of modelled containment wall mesh with studied ring section located in middle height of the containment.

4.5.2 Simulation of long-term effects

To simulate the long-term effects of shrinkage and creep after 50 years, the calculated values presented in Appendix 1 are used. The FE software ABAQUS (Brigade/Plus) provides two independent thermal expansion modules, which are utilized here to represent autogenous and drying shrinkage as well as creep by applying equivalent temperature loads. Shrinkage and creep are assumed to be independent and are therefore implemented as two separate temperature-load contributions.

Shrinkage and creep strains are calculated in accordance with Eurocode 2 and are presented in Appendix 1. In the FE model, these strains are represented by equivalent temperature loads, using a thermal expansion coefficient of $\alpha = 10^{-5}K^{-1}$. The same creep and shrinkage strains as used in the hand calculations, Figure 26 and Figure 28, are applied in the FE analysis as temperature loads on the inner and outer surfaces, creating a temperature gradient through the wall thickness.

For the outer wall, the total creep and shrinkage strain (including creep due to tendon prestressing) is approximately 470 μ-strain after 50 years. Using Equation (13), this is converted to an equivalent temperature load of −47 K. For the inner wall, the total shrinkage strain is approximately 250 μ-strain after 50 years, corresponding to an equivalent temperature load of −25 K using Equation (13).

$$\Delta T = \frac{\varepsilon}{\alpha} \qquad (13)$$

The temperature used here does not represent any physical thermal condition but is only a numerical method to introduce equivalent expansion/contraction in the concrete. In the FE model, the temperature load is applied on the surfaces and

across the entire concrete cross-section, resulting in a temperature gradient through the wall thickness that represents shrinkage and creep, as shown in Figure 31.

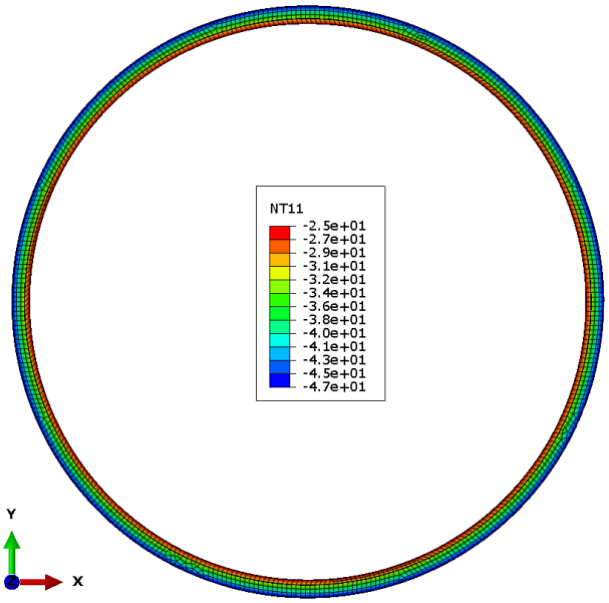

Figure 31. Shrinkage and creep applied as a temperature gradient through the containment wall, NT11 represents applied temperature in unit Kelvin.

4.5.3 Principal strain and deformation

Figure 32 shows the minimum principal strain, and Figure 33 shows the radial displacement for the long-term load case with shrinkage and creep applied. For each figure, the undeformed structure is shown in (a), and the deformed structure is shown in (b) with a scale factor of 600. The outer concrete cylinder exhibits larger negative strain and radial displacement, since the prestressing reduces its radius in combination with shrinkage.

If the cylinders were completely free to move (i.e., without the boundary conditions described in Chapter. 4.2.5), the radial displacement of the outer cylinder would reduce more than that of the inner cylinder. The strain and deformation magnitudes are summarized in Table 7. These results are compared with hand calculations and with results from similar simulations reported in the literature.

a)

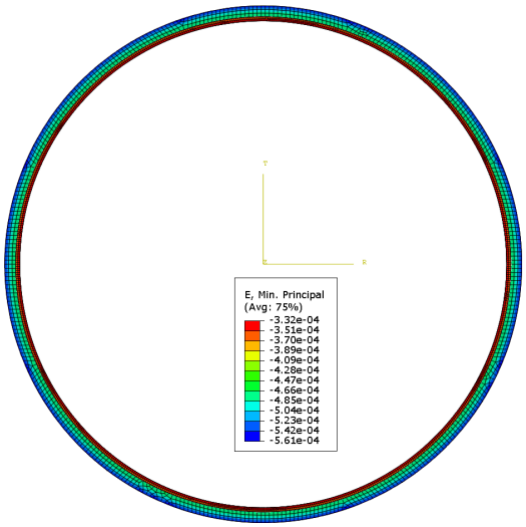

b)

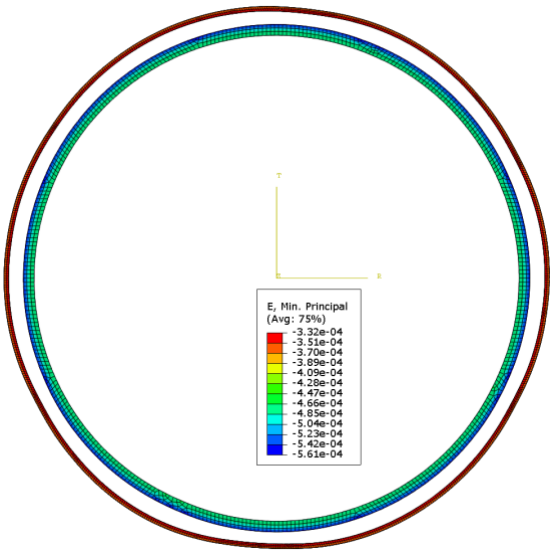

Figure 32. Creep and shrinkage strain for the containment wall middle height of reactor represented as minimum principal strain. (a) Undeformed structure; (b) deformed structure with scale factor 600 (b).

a)

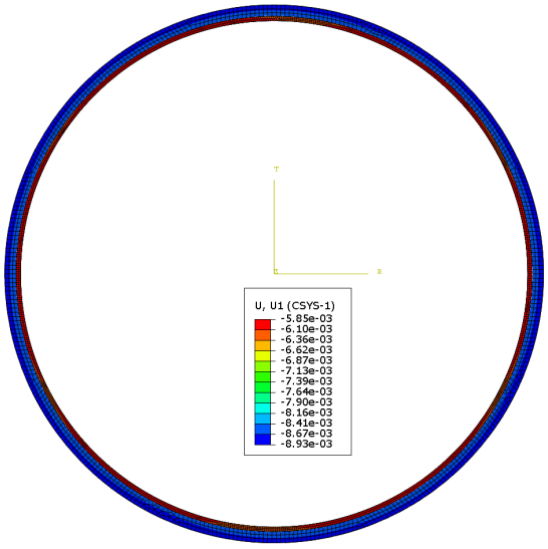

b)

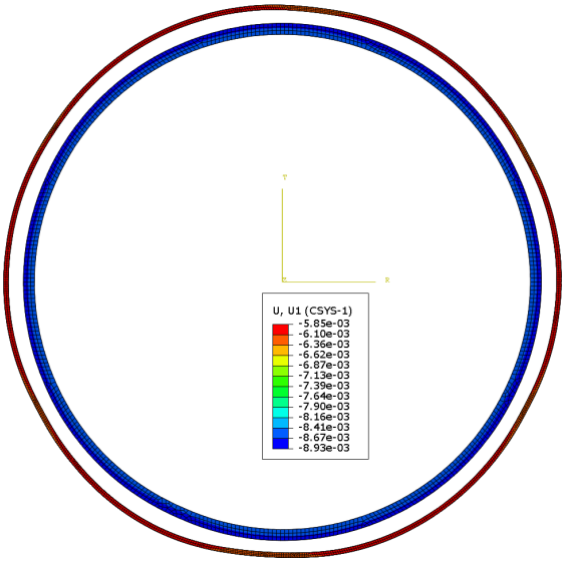

Figure 33. Radial deformation of the containment wall middle height of reactor. (a) Undeformed structure; (b) deformed structure with scale factor 600 (b).

Table 7. Average strain and deformation for the inner and outer concrete cylinders in middle section of the containment wall.

	Inner cylinder	Outer cylinder
Minimum principal strain [-]	350 µ-strain	510 µ-strain
Radial deformation [mm]	6mm	8,6mm

5 Results and discussion

This chapter presents and discusses the results obtained from the analytical calculations, finite element simulations, and literature review conducted in this study. The aim is to evaluate the risk of gap formation between the steel liner and the concrete walls in Nordic reactor containment buildings, identify the governing mechanisms, and assess the implications for structural behavior and safety.

5.1 SUMMARY OF ANALYTICAL AND NUMERICAL RESULTS

The analytical calculations based on Eurocode 2 and the finite element simulations describe the short- and long-term deformation behavior of reactor containment walls subjected to shrinkage, creep, temperature variations, and prestressing effects.

The results show that long-term deformations governed by shrinkage and creep do not pose a significant risk of gap formation between the outer containment wall and the steel liner. Due to the prestressed nature of the outer wall, the combined effects of creep and shrinkage lead to a net reduction of the outer wall radius over time, which maintains contact pressure against the steel liner. This behavior was consistently observed in both hand calculations and FE-model results, see Chapter. 4, even when accounting for tendon relaxation over a 50-year period.

For the inner containment wall, the results indicate that shrinkage may theoretically lead to a small reduction in radius relative to the steel liner. Analytical results show a long-term deformation of 4,5 mm in radial direction if the inner wall were assumed to deform freely. However, this represents a conservative upper strain on the order of 200–250 μstrain after 50 years, corresponding to a radial displacement of approximant bound. In a defect-free containment structure, the compressive action of the outer prestressed concrete wall, acting through the steel liner, is expected to close or significantly limit any such potential gap.

Overall, the results indicate that in a defect-free containment wall, long-term material effects alone are unlikely to produce gaps between the steel liner and either the inner or outer concrete walls that would compromise containment integrity.

5.2 CRUCIAL MECHANISMS FOR GAP FORMATION

Based on the literature review (Chapter 3) and the case study results, the following mechanisms are identified as the most critical contributors to gap formation:

- **Concrete shrinkage**, particularly uneven shrinkage through the wall thickness
- **Temperature variations**, inducing restrained thermal strains
- **Loss or reduction of prestressing force**, either locally or globally
- **Corrosion of the steel liner**, leading to expansion of corrosion products
- **Geometrical discontinuities**, such as cutouts for pipes, manholes, and wall openings

Among these mechanisms, shrinkage and loss of prestressing force are identified as the most relevant for explaining the gap formations observed in Swedish containment buildings during wall openings.

5.3 PREREQUISITES AND CONDITIONS FOR GAP FORMATION

5.3.1 Defect-free concrete

For a defect-free containment wall, the combined analytical and numerical results indicate a low risk of gap formation. The outer prestressed concrete wall undergoes long-term radial contraction due to shrinkage and creep, which continuously presses the steel liner inward. The steel liner, being thin and relatively flexible compared to the outer wall, is unlikely to restrain this movement.

Although the inner concrete wall may experience long-term shrinkage, its drying process is very slow due to surface coating towards the inside and steel liner towards the outer side, resulting in a high relative humidity within the wall. Measurements and literature data indicate that relative humidity remains high (70–90%) even after several decades of operation. Consequently, shrinkage strains develop slowly and remain limited in magnitude.

In summary, gap formation between the steel liner and concrete should not occur in a defect-free containment wall under normal operational and environmental conditions, nor should it affect the containment's ability to withstand internal loads.

5.3.2 Reduction of prestressing force and wall stiffness

In cases where prestressing forces are locally reduced—such as during detensioning of tendons for containment wall openings or due to tendon failure—localized deformations of the containment wall may occur. Literature data and previous numerical studies, Chapter 2.4.2, show that loss of horizontal prestressing can result in radial deformations of several millimeters in affected areas. If the loss of radial force is enough to create a gap between the steel liner and the concrete is not known.

The observed gap formations in Swedish reactors have consistently been associated with containment wall openings, where a large number of tendons were detensioned. Calculations from the steam generator replacement at Ringhals 2 in 1989 showed that gaps formed during detensioning correspond well with predicted radial deformations and were expected to close upon re-tensioning. Whether complete closure occurs in practice remains uncertain, but the results clearly indicate that temporary or permanent reductions in prestressing force significantly increase the risk of gap formation, particularly near openings.

5.4 OBSERVED GAP FORMATION DURING WALL OPENINGS

Gap formations of approximately 1–5 mm have been observed in Swedish containment buildings following the creation of large wall openings (Ringhals 2–4). These gaps were

consistently located between the inner concrete wall and the steel liner**,** while no corresponding gaps were observed between the steel liner and the outer wall. Two complementary hypotheses are proposed to explain these observations:

1. **Uneven shrinkage of the inner containment wall**
   Due to moisture gradients through the wall thickness, shrinkage strains are larger near the inner surface than near the steel liner. In an intact cylindrical wall, these stresses are restrained. When a wall opening is created and prestressing is reduced, the local stiffness decreases, allowing the inner wall to bend inward and release built-in shrinkage stresses. This bending can generate a local gap between the steel liner and the inner concrete wall.
2. **Influence of the drilling and demolition process**
   The drilling of large concrete cores introduces vibrations, local heating, and mechanical pressure on the steel liner and surrounding concrete. If drilling is performed after removal of the inner concrete wall, the steel liner may be temporarily unsupported and more susceptible to deformation. When combined with uneven shrinkage stresses, the drilling process may increase the size of an existing gap or trigger delamination at the steel–concrete interface.

While both hypotheses are consistent with observed behavior, they cannot be conclusively validated without dedicated measurements performed before, during, and after containment wall openings.

5.5 CRITICAL SECTIONS AND IMPLICATIONS FOR SAFETY

Based on the results of this study, several critical sections within reactor containment buildings have been identified where gap formation may occur and potentially affect structural integrity:

- **Closed or partially water-filled cavities** at the steel–concrete interface, where corrosion risks are elevated
- **Cutouts for pipes and manholes**, where stress concentrations and reduced interaction between steel and concrete may occur
- **Areas with significant loss of prestressing force**, leading to localized deformation and potential steel liner deformation
- **Containment wall openings**, where reduced stiffness and altered stress fields facilitate gap formation

The presence of a gap is particularly critical when it enables corrosion of the steel liner. If corrosion initiates and progresses, the expansion of corrosion products may further increase the gap, reduce liner thickness, and in severe cases compromise airtightness. However, small gaps on the order of a few millimeters, as observed in Swedish reactors, are not expected to immediately compromise containment integrity, provided that corrosion does not develop.

5.5.1 Implication on structural integrity of a gap in the reactor containment wall

The potential impact of a gap on structural integrity is difficult to quantify. In the event of an internal accident involving a rise in internal pressure, or in the case of internal missiles, a small gap between the inner containment wall and steel liner is not expected to significantly change the structural response, since the gap would likely close under internal or local pressure. In that case, the steel liner and the concrete wall would again act together as a single unit with the external wall tensioned.

For a larger gap, it is more difficult to assess the impact on the wall and the building's structural response. Within the scope of this work, this could not be evaluated further and therefore remains an open question.

5.6 OVERALL CONCLUSIONS FROM RESULTS

The combined analytical, numerical, and literature-based investigation indicates that:

- The risk of gap formation between the steel liner and concrete is low in defect-free Nordic reactor containment buildings with intact prestressing systems.
- Long-term shrinkage and creep do not lead to gap formation at the steel liner–outer wall interface and are unlikely to create significant gaps at the inner wall interface under normal conditions.
- Observed gap formations in Swedish reactors are strongly associated with containment wall openings, detensioning of tendons, and local changes in boundary conditions, rather than inherent long-term material behavior.
- Uneven shrinkage of the inner containment wall, combined with the drilling and demolition process, is the most plausible explanation for the observed gaps in Swedish reactors.
- While the observed gap magnitudes are relatively small, they may increase the risk of corrosion if environmental conditions allow, highlighting the importance of inspection and monitoring.

6 Suggestion for future work

This study has improved the understanding of gap formation between the steel liner and the concrete in cylindrical reactor containment buildings, with particular focus on Swedish reactors where gaps have been identified in connection with drilling through the containment wall. The modelling work has been limited by scarce site-specific data and by the use of simplified descriptions of drying shrinkage and creep. While the applied methods are suitable for screening and for assessing the likelihood of gap formation, further work is needed to verify mechanisms, quantify uncertainties, and strengthen conclusions for specific plants and operating histories.

The following activities are recommended to support continued development:

Targeted measurement data from observed gaps

The availability of reliable, well-documented measurements of gap formation has been limited. Future work should prioritize collecting accurate geometric data (gap width, extent, location and orientation), together with associated boundary conditions (temperature and humidity history, liner details, reinforcement arrangement, tendon forces, construction joints, and local geometry). Such datasets are essential for validating models and enabling case-specific parameter calibration.

Monitoring during detensioning and drilling activities

To assess the contribution of detensioning and drilling to gap initiation and propagation, dedicated measurement campaigns should be planned before any intervention begins. Both inner and outer sides of the containment wall should be instrumented to capture:

- local displacements and strains in concrete and liner
- tendon force changes (where relevant)
- vibration and dynamic response during drilling
- time-dependent recovery or progression after the activity

A structured measurement plan (sensor layout, sampling frequency, baseline measurements, and acceptance criteria) would significantly improve the evidential basis for conclusions.

Plant engagement and site visits

A dedicated site visit to one or more reactors where gap formation has been observed is recommended. Direct review of as-built details, maintenance and drilling procedures, environmental conditions, and inspection records would improve understanding of practical mechanisms and support selection of representative cases for modelling and monitoring.

7 References

Barslivo, G., Österberg, E., Aghili, B. (2003). *Utredning kring reaktorinneslutningar - konstruktion, skador samt kontroller och provningar.* SKI Rapport 02:58, 2003.

Berthet, J. F., Yurtdas, I., Delmas, Y., & Li, A. (2011). Evaluation of the adhesion resistance between steel and concrete by push out test. *International Journal of Adhesion and Adhesives*.

Bradford, Mark A., Oehlers, Deric J. (1995). *Composite Steel and Concrete Structural Members - Fundamental behaviour.* Pergamon.

Carlsson, S., Thelandersson, N., Ottosen, S. (1986). *Spännings och deformationsanalys av inneslutning Ringhals II - Studie av temoprär transportöppning.* Lund: Projekt. RÅG, BIT-651196, 1986.

CEN, E. C. (2014). *EN 1992-1-1: Eurocode 2: Design of concrete structures — Part 1-1: General rules and rules for buildings.* CEN.

Gasch, T., Ahmed, L., Malm, R. (2018). *Instrumentation and Modelling of a Reactor Containment Building.* Energiforsk Report 2018:526, 2018.

Hassanzadeh, M., Malm, R., Åhs, M. (2018). *Reaktorinneslutningarnas respons vid höga inre tryck och reducerad förspänning.* Strålsäkerhetsmyndigheten Rapport 2018:26, 2018.

Lundqvist, P. (2012). *Assessment of Long-Term Losses in Prestressed Concrete Structures - Application for Nuclear Reactor Containments.* Elforsk Rapport 12:74, 2012.

Malm, R., Åhs, M., Hassanzadeh, M. (2021). *Syretransport genom reaktorinneslutningar och korrosion av ingjutna tätplåtar.* Energiforsk rapport 2021:786, 2021.

Teollisuuden Voima Oy. (2008). *Nuclear power plant units: Olkiluoto 1 and Olkiluoto 2.* Teollisuuden Voima Oy, 2008.

Oxfall, M. (2016). *Climatic conditions inside nuclear reactor containments: Evaluation of moisture condition in the concrete within reactor containments and interaction with the ambient compartments, PHD thesis.* Lund University, 2016.

Oxfall, M. (2017). *Simulerad uttorkning av betong i reaktorinneslutningar.* Energiforsk Rapport 2017:464.

Roth, T., Silfwerbrand, J., Sundquist, H. (2002). *Betonginneslutningar i svenska kärnkraftverk - En sammanställning över konstruktion och material.* Stockholm: SKI Rapport 02:59, 2002.

Sandberg, B., Sederholm, B., Taxen, C., Trägårdh, J., Tidblad, T. (2019). *Genomgång av potentiella korrosionsrisker för ingjuten tätplåt i reaktorinneslutningar.* Energiforsk Rapport 2019:581, 2019.

Zaraei, N., Lundqvist, P. (2021). *Compilation of Concrete Test Data from The Nuclear Industry.* Energiforsk Report 2021:761, 2021.

8 Appendix A: Hand calculations – Creep and shrinkage

Appendix A presents hand calculations for the case study presented in Chapter. 4.

Calculations are presented for creep, page 1, shrinkage, page 2 and resulting creep strain from prestressing force acting on the outer cylindrical concrete wall, page 3.

Creep calculations: Inner and outer containment wall

According to SS-EN 1992-1-1, 3.1.4/ Appendix B

Inner containment wall:

Data	**Remark**	**t = 28 days**	**t = 365 days**	**t = 18250 days (50 years)**
A_c	[mm^2]	300000	300000	300000
u	[mm]	1000	1000	1000
f_{cm}	[MPa]	43	43	43
RH	[%]	90	80	70
t_0	[Dagar]	7	7	7
Life-length class:		L100	L100	L100
Result				
$\varphi(t,t_0)$	Creep number, B.1	**1.72**	**1.88**	**2.04**
Part results				
φ_0	B.2	1.720	1.881	2.041
φ_{RH}	B.3a, B.3b	1.058	1.157	1.255
$\beta(f_{cm})$	B.4	2.562	2.562	2.562
$\beta(t_0)$	B.5	0.635	0.635	0.635
h_0	[mm] B.6	600	600	600
$\beta_c(t,t_0)$	B.7	1.0000	1.0000	1.0000
β_H	B.8a, B.8b	1353.3	1353.3	1164.6
α_1	B.8c	0.866	0.866	0.866
α_2	B.8c	0.960	0.960	0.960
α_3	B.8c	0.902	0.902	0.902
t	[Days]	28	365	18250

Outer containment wall:

Data	**Remark**	**t = 28 days**	**t = 365 days**	**t = 18250 days (50 years)**
A_c	[mm^2]	800000	800000	800000
u	[mm]	1000	1000	1000
f_{cm}	[MPa]	43	43	43
RH	[%]	90	85	80
t_0	[Dagar]	7	7	7
Life-length class:		L100	L100	L100
Result				
$\varphi(t,t_0)$	Creep number, B.1	**1.68**	**1.73**	**1.79**
Part results				
φ_0	B.2	1.676	1.734	1.791
φ_{RH}	B.3a, B.3b	1.031	1.066	1.102
$\beta(f_{cm})$	B.4	2.562	2.562	2.562
$\beta(t_0)$	B.5	0.635	0.635	0.635
h_0	[mm] B.6	1600	1600	1600
$\beta_c(t,t_0)$	B.7	1.0000	1.0000	1.0000
β_H	B.8a, B.8b	1353.3	1353.3	1353.3
α_1	B.8c	0.866	0.866	0.866
α_2	B.8c	0.960	0.960	0.960
α_3	B.8c	0.902	0.902	0.902
t	[Days]	28	365	18250

Shrinkage calculations: Inner and outer containment wall

According to SS-EN 1992-1-1, 3.1.4/ Appendix B

Inner containment wall:

Data	**Remark**	**t = 28 days**	**t = 365 days**	**t = 18250 days (50 years)**
A_c	[mm^2]	300000	300000	300000
u	[mm]	1000	1000	1000
f_{ck}	[MPa]	40	40	40
f_{cm}	[MPa]	48	48	48
RH	[%]	90	80	70
t_s	[Days]	7	7	7
Cement grade:	3.1.2. (6)	S	S	S
Life length grade:		L100	L100	L100
Result				
ε_{cs}	[‰]	0.149	0.208	0.254
Part results				
Drying shrinkage:				
$\varepsilon_{cd,0}$	B.11	0.000105	0.000189	0.000255
β_{RH}	B.12	0.42005	0.7564	1.0184
f_{cmo}	[MPa]	10	10	10
α_{ds1}		3	3	3
α_{ds2}		0.13	0.13	0.13
RH_0	[%]	100	100	100
h_0	[mm] B.6	600	600	600
k_h	Table 3.3	0.70	0.70	0.70
t	[Days]	28	365	18250
ε_{cd} (t)	3.9	0.0000737	0.0001326	0.0001786
β_{ds} (t,t_s)	3.10	1.000000	1.000000	1.000000
Autogenous shrinkage:				
ε_{ca} (t)	3.11	0.000075	0.000075	0.000075
ε_{ca} (∞)	3.12	0.000075	0.000075	0.000075
β_{as} (t)	3.13	1.000	1.000	1.000

Outer containment wall:

Data	**Remark**	**t = 28 days**	**t = 365 days**	**t = 18250 days (50 years)**
A_c	[mm^2]	800000	800000	800000
u	[mm]	1000	1000	1000
f_{ck}	[MPa]	40	40	40
f_{cm}	[MPa]	48	48	48
RH	[%]	90	85	80
t_s	[Days]	7	7	7
Cement grade:	3.1.2. (6)	S	S	S
Life length grade:		L100	L100	L100
Result				
ε_{cs}	[‰]	0.149	0.180	0.208
Part results				
Drying shrinkage:				
$\varepsilon_{cd,0}$	B.11	0.000105	0.000150	0.000189
β_{RH}	B.12	0.42005	0.5981	0.7564
f_{cmo}	[MPa]	10	10	10
α_{ds1}		3	3	3
α_{ds2}		0.13	0.13	0.13
RH_0	[%]	100	100	100
h_0	[mm] B.6	1600	1600	1600
k_h	Table 3.3	0.70	0.70	0.70
t	[Days]	28	365	18250
ε_{cd} (t)	3.9	0.0000737	0.0001049	0.0001326
β_{ds} (t,t_s)	3.10	1.000000	1.000000	1.000000
Autogenous shrinkage:				
ε_{ca} (t)	3.11	0.000075	0.000075	0.000075
ε_{ca} (∞)	3.12	0.000075	0.000075	0.000075
β_{as} (t)	3.13	1.000	1.000	1.000

Post-tensioned tendons

According to SS-EN 1992-1-1 3.1.4 with modified modulus of elasticity

Horizontally

E_{cm}	3.50E+10	
$\phi(28d,t_0)$	1.68	Creep 28 days
$\phi(365d,t_0)$	1.73	Creep 365 days
$\phi(50y,t_0)$	1.79	Creep 50 years

For loads with a duration that induces creep, the total deformation including creep may be calculated by using an effective elasticity modulus for concrete.

$E_{c.eff}$	$E_{cm}/(1+\phi(\infty,t0))$	
$E_{c.eff}.28d$	1.31E+10	Effective elasticity modulus of concrete after 28 days.
$E_{c.eff}.365d$	1.28E+10	Effective elasticity modulus of concrete after 365 days.
$E_{c.eff}.50y$	1.25E+10	Effective elasticity modulus of concrete after 50 years.

σ_p	1.20E+09	Initial post-tensioning stress [Pa]
n_p	3	Number of tendons per meter section

The concrete is compressed with a strain corresponding to the stress on the concrete section.

σ_{sw}	0	Self weight per meter section [Pa]
$\sigma_{p.s}$	3.60E+09	Initial post-tensioning stress per meter section [Pa]
$\Delta\sigma_{pr}$	0.025	Loss in prestress is approximated from EC2 to a relaxation loss of 2,5%
$\varepsilon_{btg.init}$	0.000	Initial strain per meter section - 28 days
$\varepsilon_{btg.tens}$	0.281	Strain per meter section - 365 days
$\varepsilon_{btg.end}$	0.280	Strain per meter section - 50 years

GAP FORMATION BETWEEN STEEL LINER AND CYLINDER WALL IN REACTOR CONTAINMENT BUILDINGS

The reactor containment building is the most important safety barrier in a nuclear power plant. It is a cylindrical, prestressed concrete structure with an embedded steel liner on the inner face of the containment wall, designed to maintain integrity in the event of an internal accident.

In Sweden, holes have been drilled through the containment walls of four reactors. Following drilling, gaps were observed between the inner concrete surface and the steel liner. Such gaps may adversely affect containment performance by altering its mechanical behavior under accident loading.

This report suggests that the observed gap formation between the steel liner and the inner concrete wall is a consequence of uneven shrinkage effect together with the hole making process of drilling and releasing of prestressing force. Furthermore, the conclusion that in a defect free concrete the risk of gap formation in a concrete containment wall with a steel liner embedded is low.

Another step forward in Swedish energy research

Energiforsk – Swedish Energy Research Centre is a research and knowledge based organization that brings together large parts of Swedish research and development on energy. The goal is to increase the efficiency and implementation of scientific results to meet future challenges in the energy sector. We work in a number of research areas such as hydropower, energy gases and liquid automotive fuels, fuel based combined heat and power generation, and energy management in the forest industry. Our mission also includes the generation of knowledge about resource-efficient sourcing of energy in an overall perspective, via its transformation and transmission to its end-use.
Read more: www.energiforsk.se

Energiforsk